TTP06-31
hep-ph/0612167
December 2006

Theoretical update of $B_s - \overline{B}_s$ mixing

ALEXANDER LENZ
Institut für Theoretische Physik – Universität Regensburg
D-93040 Regensburg, Germany

and

ULRICH NIERSTE
Institut für Theoretische Teilchenphysik – Universität Karlsruhe
D-76128 Karlsruhe, Germany

Abstract

We update the theory predictions for the mass difference ΔM_s, the width difference $\Delta\Gamma_s$ and the CP asymmetry in flavour-specific decays, $a^s_{\rm fs}$, for the $B_s - \overline{B}_s$ system. In particular we present a new expression for the element Γ^s_{12} of the decay matrix, which enters the predictions of $\Delta\Gamma_s$ and $a^s_{\rm fs}$. To this end we introduce a new operator basis, which reduces the troublesome sizes of the $1/m_b$ and α_s corrections and diminishes the hadronic uncertainty in $\Delta\Gamma_s/\Delta M_s$ considerably. Logarithms of the charm quark mass are summed to all orders. We find $\Delta\Gamma_s/\Delta M_s = (49.7 \pm 9.4)\cdot 10^{-4}$ and $\Delta\Gamma_s = (f_{B_s}/240\,\text{MeV})^2[(0.105 \pm 0.016)\,B + (0.024 \pm 0.004)\,\tilde{B}'_S - 0.027 \pm 0.015]\,\text{ps}^{-1}$ in terms of the bag parameters B, $\tilde{B}'_S$ in the NDR scheme and the decay constant f_{B_s}. The improved result for Γ^s_{12} also permits the extraction of the CP-violating $B_s - \overline{B}_s$ mixing phase from $a^s_{\rm fs}$ with better accuracy. We show how the measurements of ΔM_s, $\Delta\Gamma_s$, $a^s_{\rm fs}$, $A^{\rm mix}_{\rm CP}(B_s \to J/\psi\phi)$ and other observables can be efficiently combined to constrain new physics. Applying our new formulae to data from the DØ experiment, we find a 2σ deviation of the $B_s - \overline{B}_s$ mixing phase from its Standard Model value. We also briefly update the theory predictions for the $B_d - \overline{B}_d$ system and find $\Delta\Gamma_d/\Delta M_d = \left(52.6^{+11.5}_{-12.8}\right)\cdot 10^{-4}$ and $a^d_{\rm fs} = \left(-4.8^{+1.0}_{-1.2}\right)\cdot 10^{-4}$ in the Standard Model.

PACS numbers: 12.38.Bx, 13.25.Hw, 11.30Er, 12.60.-i

1 Introduction

Flavour-changing neutral current (FCNC) processes are highly sensitive to new physics around the TeV scale. Global fits to the unitarity triangle show an excellent agreement of $b \to d$ and $s \to d$ transitions with the predictions of the Cabibbo-Kobayashi-Maskawa (CKM) mechanism [1,2]. Extensions of the Standard Model can contain sources of flavour-changing transitions beyond the CKM matrix. Models without these new sources are termed to respect *minimal flavour violation (MFV)*. Despite of the success of the MFV hypothesis in $b \to d$ and $s \to d$ transitions there is still sizable room for non-MFV contribution in $b \to s$ transitions. For instance, an extra contribution to $b \to s\overline{q}q$, $q = u, d, s$, decay amplitudes with a CP phase different from $\arg(V_{ts}^* V_{tb})$ can alleviate the $\sim 2.6\sigma$ discrepancy between the measured mixing-induced CP asymmetries in these $b \to s$ penguin modes and the Standard Model prediction [3]. Models of supersymmetric grand unification can naturally accommodate new contributions to $b \to s$ transitions [4]: right-handed quarks reside in the same quintuplets of SU(5) as left-handed neutrinos, so that the large atmospheric neutrino mixing angle could well affect squark-gluino mediated $b \to s$ transitions [5].

Clearly, $B_s - \overline{B}_s$ mixing plays a preeminent role in the search for new physics in $b \to s$ FCNC's. $B_s - \overline{B}_s$ oscillations are governed by a Schrödinger equation

$$i\frac{d}{dt}\begin{pmatrix} |B_s(t)\rangle \\ |\bar{B}_s(t)\rangle \end{pmatrix} = \left(M^s - \frac{i}{2}\Gamma^s\right)\begin{pmatrix} |B_s(t)\rangle \\ |\bar{B}_s(t)\rangle \end{pmatrix} \tag{1}$$

with the mass matrix M^s and the decay matrix Γ^s. The physical eigenstates $|B_H\rangle$ and $|B_L\rangle$ with the masses M_H, M_L and the decay rates Γ_H, Γ_L are obtained by diagonalizing $M^s - i\Gamma^s/2$. The $B_s - \overline{B}_s$ oscillations in Eq. (1) involve the three physical quantities $|M_{12}^s|$, $|\Gamma_{12}^s|$ and the CP phase $\phi_s = \arg(-M_{12}^s/\Gamma_{12}^s)$ (see e.g. [6]). The mass and width differences between B_L and B_H are related to them as

$$\Delta M_s \;=\; M_H^s - M_L^s \;=\; 2\,|M_{12}^s|, \qquad \Delta\Gamma_s \;=\; \Gamma_L^s - \Gamma_H^s \;=\; 2\,|\Gamma_{12}^s|\cos\phi_s, \tag{2}$$

up to numerically irrelevant corrections of order m_b^2/M_W^2. ΔM_s simply equals the frequency of the $B_s - \overline{B}_s$ oscillations. A third quantity providing independent information on the mixing problem in Eq. (1) is

$$a_{\rm fs}^s \;=\; \mathrm{Im}\,\frac{\Gamma_{12}^s}{M_{12}^s} \;=\; \frac{|\Gamma_{12}^s|}{|M_{12}^s|}\sin\phi_s \;=\; \frac{\Delta\Gamma_s}{\Delta M_s}\tan\phi_s. \tag{3}$$

$a_{\rm fs}^s$ is the CP asymmetry in *flavour-specific* $B_s \to f$ decays, which means that the decays $\overline{B}_s \to f$ and $B_s \to \overline{f}$ (with $\overline{f}$ denoting the CP-conjugate final state) are forbidden [7]. The standard way to access $a_{\rm fs}^s$ uses $B_s \to X_s\ell^+\overline{\nu_\ell}$ decays, which justifies the name *semileptonic CP asymmetry* for $a_{\rm fs}^s$. (See e.g. [6, 8] for more details on the phenomenology of $B_s - \overline{B}_s$ mixing.)

It is important to note that new physics can significantly affect M_{12}^s, but not Γ_{12}^s, which is dominated by the CKM-favoured $b \to c\overline{c}s$ tree-level decays. Hence all possible effects of new physics can be parameterised by two real parameters only, for instance $|M_{12}^s|$ and ϕ_s. While

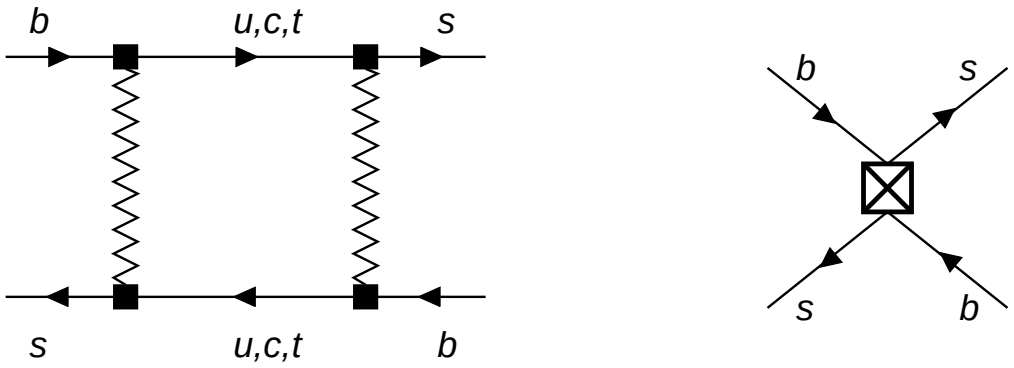

Figure 1: In the lowest order M_{12}^s is calculated from the dispersive parts of the box diagrams on the left. It is dominated by the top contribution. The result involves only one local $|\Delta B| = 2$ operator, shown in the right picture. The leading contribution to Γ_{12}^s is obtained from the absorptive parts of the box diagrams on the left, to which only diagrams without top quark line contribute. To lowest order in the heavy quark expansion two $|\Delta B| = 2$ operators occur, the $\overline{\Lambda}/m_b$ corrections involve five more.

$|M_{12}^s|$ is directly related to ΔM_s, the extraction of ϕ_s from either $\Delta\Gamma_s$ or $a_{\rm fs}^s$ requires an accurate knowledge of Γ_{12}^s.

In the Standard Model M_{12}^s and Γ_{12}^s are computed from the box diagrams in Fig. 1 and QCD corrections in the desired order. The Standard Model prediction for M_{12} reads:

$$M_{12} \;=\; \frac{G_F^2 M_{B_s}}{12\pi^2}\, M_W^2\, (V_{tb}V_{ts}^*)^2\, \widehat{\eta}_B\, S_0(x_t)\, f_{B_s}^2 B, \tag{4}$$

where G_F is the Fermi constant, the V_{ij}'s are CKM elements, M_{B_s} and M_W are the masses of B_s meson and W boson and the short-distance information is contained in $\widehat{\eta}_B\, S_0(x_t)$: $S_0(x_t)$ is the Inami-Lim function, which depends on the top mass m_t through $x_t = m_t^2/M_W^2$, and $\widehat{\eta}_B$ is a numerical factor containing the leading and next-to-leading QCD corrections [9]. The calculation of M_{12} involves the four-quark operator ($\alpha, \beta = 1, 2, 3$ are colour indices):

$$Q \;=\; \overline{s}_\alpha \gamma_\mu (1-\gamma_5) b_\alpha\, \overline{s}_\beta \gamma^\mu (1-\gamma_5) b_\beta. \tag{5}$$

All long-distance QCD effects are contained in the hadronic matrix element of Q and are parameterised by $f_{B_s}^2 B$:

$$\langle B_s | Q | \overline{B}_s \rangle \;=\; \frac{8}{3} M_{B_s}^2\, f_{B_s}^2 B. \tag{6}$$

The recent observation of the $B_s - \overline{B}_s$ mixing frequency $\Delta M_s = 2|M_{12}^s|$ at the Tevatron [10] yields a powerful constraint on extensions of the Standard Model [11–14]. The results from the DØ and CDF experiments obtained with 1 fb^{-1} of data, are [15]

$$\begin{aligned} 17\,\text{ps}^{-1} \le \Delta M_s &\le 21\,\text{ps}^{-1} && @90\%\,\text{CL} && \text{DØ} \\ \Delta M_s &= 17.77 \pm 0.10_{\text{(syst)}} \pm 0.07_{\text{ (stat)}}\,\text{ps}^{-1} && && \text{CDF}. \end{aligned} \tag{7}$$

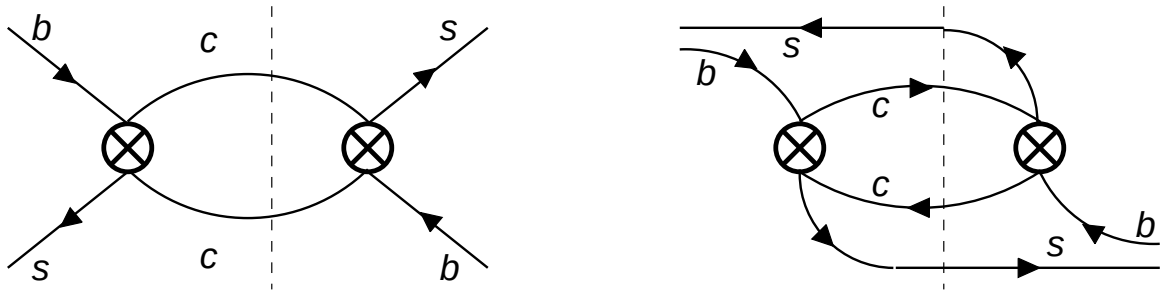

Figure 2: Leading-order CKM-favoured contribution to Γ_{12}^s, which arises from $\overline{(B}_s)$ decays to final states (indicated by the dashed lines) with a $(c, \overline{c})$ pair and zero strangeness. The crosses denote any of the operators Q_{1-6} of the $|\Delta B| = 1$ hamiltonian. The Cabibbo-suppressed contributions correspond to diagrams with one or both c quarks replaced by u quarks.

While the precise measurement in Eq. (7) sharply determines $|M_{12}^s|$, the uncertainty of $f_{B_s}^2 B$, which is around 30%, blurs the extraction of some new physics contribution adding to $S_0(x_t)$ in Eq. (4). Alternatively one can study the ratio $\Delta M_d/\Delta M_s$, where ΔM_d is the mass difference in the $B_d - \overline{B}_d$ system. While the hadronic uncertainty in the ratio $f_{B_s}^2 B/(f_{B_d}^2 B_{B_d})$ is smaller, one is now dependent on $|V_{td}/V_{ts}|^2$. Even if one assumes non-standard contributions only in B_s physics, but not in the quantities entering the global fit of the unitarity triangle, $|V_{td}/V_{ts}|^2$ is only known to roughly 40% [2] leaving equally much room for new physics in $|M_{12}^s|$.

Adding experimental information from $\Delta\Gamma_s$ or $a_{\rm fs}^s$ helps in two ways; first, one can study the CP-violating phase ϕ_s, which is totally unconstrained by ΔM_s, through Eqs. (2) and (3). Second, one expects cancellations of hadronic parameters in the ratio Γ_{12}^s/M_{12}^s, which enters $a_{\rm fs}^s$ and $\Delta\Gamma_s/\Delta M_s$. All decays into final states with zero strangeness contribute to Γ_{12}^s, which is dominated by the CKM-favoured $b \to c\overline{c}s$ tree-level contribution. In the first step of the calculation the W-boson is integrated out and the W-mediated $|\Delta B| = 1$ transitions are described by the usual effective $|\Delta B| = 1$ hamiltonian with the current-current operators Q_1, Q_2 and the penguin operators Q_{3-6}, Q_8 [16]. The leading contribution to Γ_{12}^s in this effective $|\Delta B| = 1$ theory is shown in Fig. 2. In the second step one uses an operator product expansion (OPE), the Heavy Quark Expansion (HQE), to express Γ_{12}^s as an expansion in the two parameters $\overline{\Lambda}/m_b$ and $\alpha_s(m_b)$. Here α_s is the QCD coupling constant and $\overline{\Lambda}$ is the appropriate hadronic scale, which quantifies the size of the hadronic matrix elements. The HQE links the diagrams of Fig. 2 to the matrix elements of local $\Delta B = 2$ operators. In addition to the operator Q in Eq. (5) one also encounters

$$Q_S \;=\; \overline{s}_\alpha(1+\gamma_5)b_\alpha\,\overline{s}_\beta(1+\gamma_5)b_\beta, \tag{8}$$

whose matrix element is parameterised by a bag parameter B_S in analogy to Eq. (6). The leading contribution to Γ_{12}^s was obtained in [7, 17]. Today Γ_{12}^s is known to next-to-leading-order (NLO) in both $\overline{\Lambda}/m_b$ [18] and $\alpha_s(m_b)$ [19, 20]. The 1998 result [19]

$$\left(\frac{\Delta\Gamma_s}{\Gamma_s}\right) = \left(\frac{f_{B_s}}{210\ \text{MeV}}\right)^2 [0.006\,B + 0.150\,B_S - 0.063] \tag{9}$$

with the average total width $\Gamma_s = (\Gamma_L^s + \Gamma_H^s)/2$ is pathological in several respects: first, the $\overline{\Lambda}/m_b$ correction -0.063 is unnaturally large and amounts to around 40% of the total result. Second, the coefficient of B cancels almost completely, the result is therefore dominated by the term proportional to $B_S \sim 0.9$, so that the cancellation of hadronic quantities from the ratio $\Delta\Gamma_s/\Delta M_s$ is very imperfect. Third, both the $\overline{\Lambda}/m_b$ and α_s corrections, which diminish the coefficient of B_S from 0.22 to 0.15, are negative, and these numerical cancellations between leading-order (LO) order result and corrections increase the relative uncertainty of the prediction for $\Delta\Gamma_s/\Gamma_s$. In the following section we argue that these pathologies are caused by a poor choice of the operator basis used in [18–20] and propose a different basis. We also improve the prediction of $\Delta\Gamma_s/\Delta M_s$ and $\Delta\Gamma_s/\Gamma_s$ in several other aspects, by summing logarithms of the charm mass to all orders in α_s, by using different renormalisation schemes for the b-quark mass, by including CKM-suppressed contributions and by modifying the normalisation related to the factor $1/\Gamma_s$ in Eq. (9). In Sect. 3 we present numerical updates first of ΔM_s, $\Delta\Gamma_s$ and $a_{\rm fs}^s$ and then of the corresponding quantities in the B_d-system. In Sect. 4 we show how the expressions for the mixing quantities change in the presence of new physics. Here we discuss how to combine different present and future measurements to constrain $|M_{12}^s|$ and ϕ_s and advocate a novel method to display the constraints on possible new short-distance physics in $B_s - \overline{B}_s$ mixing. Sect. 5 gives a road map for future measurements and calculations and Sect. 6 summarises our results.

2 Improved prediction of Γ_{12}^s

We write Γ_{12}^s as [21]

$$\Gamma_{12}^s = -\Big[\lambda_c^2\,\Gamma_{12}^{cc} + 2\,\lambda_c\,\lambda_u\,\Gamma_{12}^{uc} + \lambda_u^2\,\Gamma_{12}^{uu}\Big] \tag{10}$$

$$= -\Big[\lambda_t^2\,\Gamma_{12}^{cc} + 2\,\lambda_t\,\lambda_u\,(\Gamma_{12}^{cc} - \Gamma_{12}^{uc}) + \lambda_u^2\,(\Gamma_{12}^{cc} - 2\Gamma_{12}^{uc} + \Gamma_{12}^{uu})\Big] \tag{11}$$

with the CKM factors $\lambda_i = V_{is}^* V_{ib}$ for $i = u, c, t$. In Eq. (11) we have eliminated λ_c in favour of λ_t using $\lambda_u + \lambda_c + \lambda_t = 0$ to prepare for the study of Γ_{12}^s/M_{12}^s. Since $|\lambda_u| \ll |\lambda_t| \approx |\lambda_c|$, Γ_{12}^{cc} clearly dominates Γ_{12}^s. For $ab = cc, uc, uu$ we write [19, 21]

$$\Gamma_{12}^{ab} = \frac{G_F^2 m_b^2}{24\pi\, M_{B_s}}\Big[G^{ab}\,\langle B_s|Q|\overline{B}_s\rangle - G_S^{ab}\,\langle B_s|Q_S|\overline{B}_s\rangle\Big] + \Gamma_{12,1/m_b}^{ab} \tag{12}$$

The coefficients G^{ab} and G_S^{ab} are further decomposed as

$$G^{ab} = F^{ab} + P^{ab}, \qquad G_S^{ab} = -F_S^{ab} - P_S^{ab}. \tag{13}$$

Here F^{ab} and F_S^{ab} are the contributions from the current-current operators $Q_{1,2}$ while the small coefficients P^{ab} and P_S^{ab} stem from the penguin operators Q_{3-6} and Q_8. (Note that in [19], where only the dominant Γ_{12}^{cc} was considered, these coefficients had no superscript 'cc'.) Numerical cancellations render F^{cc} small with $|F^{cc}/F_S^{cc}| \approx 0.03$ which explains the small coefficient of B in Eq. (9).

We parameterise the matrix element of Q_S as

$$\langle B_s|Q_S|\overline{B}_s\rangle \;=\; -\frac{5}{3}M_{B_s}^2\, f_{B_s}^2\, B_S'. \tag{14}$$

Formulae for physical quantities are more compact when expressed in terms of B_S' rather than the conventionally used bag parameter B_S. The two parameters are related as

$$B_S' \;=\; \frac{M_{B_s}^2}{(\overline{m}_b+\overline{m}_s)^2}B_S. \tag{15}$$

In the vacuum insertion approximation (VIA) the bag factors B and B_S are equal to one. Throughout this paper we use the $\overline{\rm MS}$ scheme as defined in [19,21] for all operators. Therefore the masses $\overline{m}_b$ and $\overline{m}_s$ appearing in Eq. (15) correspond to the $\overline{\rm MS}$ scheme as well.

$\Gamma_{12,1/m_b}^{cc}$ comprises effects suppressed by $\overline{\Lambda}/m_b$. We will discuss it later, after transforming to our new operator basis.

2.1 New operator basis

When calculating Γ_{12} to leading order in $\overline{\Lambda}/m_b$, one first encounters a third operator $\widetilde{Q}_S$ in addition to Q and Q_S defined in Eqs. (5) and (8):

$$\widetilde{Q}_S \;=\; \overline{s}_\alpha(1+\gamma_5)b_\beta\,\overline{s}_\beta(1+\gamma_5)b_\alpha, \tag{16}$$

However, a certain linear combination of Q, Q_S and $\widetilde{Q}_S$ is a $1/m_b$–suppressed operator [18]. This $1/m_b$–suppressed operator reads

$$R_0 \;\equiv\; Q_S \;+\; \alpha_1\tilde{Q}_S \;+\; \frac{1}{2}\alpha_2 Q, \tag{17}$$

where $\alpha_{1,2}$ contain NLO corrections, which are specific to the $\overline{\rm MS}$ scheme used by us [19]:

$$\alpha_1 \;=\; 1 \;+\; \frac{\alpha_s(\mu_2)}{4\pi}\,C_f\left(12\ln\frac{\mu_2}{m_b}+6\right), \qquad \alpha_2 \;=\; 1 \;+\; \frac{\alpha_s(\mu_2)}{4\pi}\,C_f\left(6\ln\frac{\mu_2}{m_b}+\frac{13}{2}\right). \tag{18}$$

Here $C_f=4/3$ is a colour factor and μ_2 is the scale at which the operators in Eq. (17) are defined. The coefficients G and G_S in Eq. (12) depend on μ_2 and this dependence cancels with the μ_2–dependence of $\langle B_s|Q(\mu_2)|\overline{B}_s\rangle$ and $\langle B_s|Q_S(\mu_2)|\overline{B}_s\rangle$. In lattice computations the μ_2–dependence enters in the lattice–continuum matching of these matrix elements. In our numerics we will always quote the results for $\mu_2=m_b$. In [18–20] Eq. (17) has been used to eliminate Q_S in favour of R_0 leading to the result in Eq. (9). The matrix element of $\widetilde{Q}_S$ reads

$$\langle B_s|\widetilde{Q}_S(\mu_2)|\overline{B}_s\rangle \;=\; \frac{1}{3}M_{B_s}^2\, f_{B_s}^2\,\widetilde{B}_S'(\mu_2). \tag{19}$$

In analogy to Eq. (15) we define

$$\widetilde{B}_S'(\mu_2) \;=\; \frac{M_{B_s}^2}{(\overline{m}_b(\mu_2)+\overline{m}_s(\mu_2))^2}\widetilde{B}_S(\mu_2). \tag{20}$$

For clarity we have explicitly shown the μ_2-dependence in Eqs. (19) and (20), which was skipped in Eqs. (6),(14) and (15). In VIA $\widetilde{B}_S = 1$ and $\langle B_s|\widetilde{Q}_S|\overline{B}_s\rangle$ is much smaller than $\langle B_s|Q|\overline{B}_s\rangle$ and $\langle B_s|Q_S|\overline{B}_s\rangle$. The small coefficient $1/3$ in Eq. (19) is the consequence of a cancellation between the leading term in the $1/N_c$ expansion, where $N_c = 3$ is the number of colours, and the factorisable $1/N_c$ corrections: $1/3 = 1 - 2/N_c$. One naturally expects that the bag factor $\widetilde{B}_S$ substantially deviates from 1. However, a lattice computation found $\widetilde{B}_S = 0.91 \pm 0.08$ [22], showing that the matrix element of $\widetilde{Q}_S$ is indeed small. Thus $\langle B_s|R_0|\overline{B}_s\rangle = \overline{\Lambda}/m_b$ implies a strong numerical relationship between B and B_S which can be used to constrain B_S/B entering $\Delta\Gamma_s/\Delta M_s$. Yet it is more straightforward to use Eq. (17) to eliminate Q_S altogether from Γ_{12} in favour of $\widetilde{Q}_S$. The coefficient of B will change and and the coefficient of $\widetilde{B}'_S$ is expected to be small in view of the factor of 1/3 in Eq. (19). Using further the bag parameters of Eqs. (6) and (14), Γ_{12}^{ab} of Eq. (12) now reads

$$\Gamma_{12}^{ab} \;=\; \frac{G_F^2 m_b^2}{24\pi}\, M_{B_s}\, f_{B_s}^2 \,\left[\left(G^{ab} + \frac{\alpha_2}{2} G_S^{ab}\right)\frac{8}{3} B \;+\; G_S^{ab}\alpha_1 \frac{1}{3}\widetilde{B}'_S\right] \;+\; \widetilde{\Gamma}_{12,1/m_b}^{ab}. \qquad (21)$$

The new $1/m_b$–corrections are related to $\Gamma_{12,1/m_b}^{ab}$ appearing in Eq. (12) as

$$\widetilde{\Gamma}_{12,1/m_b}^{ab} \;=\; \Gamma_{12,1/m_b}^{ab} \;+\; \frac{G_F^2 m_b^2}{24\pi\, M_{B_s}}\, F_S^{ab,(0)}\, \langle B_s|R_0|\overline{B}_s\rangle. \qquad (22)$$

Here we have taken into account that the result of [19, 20] includes the $\overline{\Lambda}/m_b$ terms without penguin contributions and to LO in α_s: consequently we have changed $-G_S^{ab}$ to $F_S^{ab,(0)}$, which is the LO approximation to F_S^{ab}. Recalling $|G^{ab}| \ll |G_S^{ab}|$ and $B, \widetilde{B}'_S \approx 1$ one easily verifies from Eq. (21) that the first term proportional to B dominates over the second term. Since $\Gamma_{12,1/m_b}^{ab}$ in Eq. (9) is negative and the shift in Eq. (22) adds a positive term our change of basis also leads to $|\widetilde{\Gamma}_{12,1/m_b}^{ab}| < |\Gamma_{12,1/m_b}^{ab}|$. Further the α_s-corrections contained in $\alpha_{1,2}$, which multiply $G_S^{ab,(0)}$ in Eq. (21), temper the large NLO corrections of the old result. These three effects combine to reduce the hadronic uncertainty in $\Delta\Gamma_s/\Delta M_s$ substantially. In other words: the uncertainty quoted in [19, 20] is not intrinsic to $\Delta\Gamma_s/\Delta M_s$ but an artifact of a poorly chosen operator basis.

2.2 A closer look at $1/m_b$ corrections

At order $1/m_b$ one encounters the operators R_0 of Eq. (17),

$$\begin{aligned} R_1 &= \frac{m_s}{m_b}\,\overline{s}_\alpha(1+\gamma_5)b_\alpha\,\overline{s}_\beta(1-\gamma_5)b_\beta \\ R_2 &= \frac{1}{m_b^2}\,\overline{s}_\alpha \overleftarrow{D}_\rho\gamma^\mu(1-\gamma_5)D^\rho b_\alpha\,\overline{s}_\beta\gamma_\mu(1-\gamma_5)b_\beta \\ R_3 &= \frac{1}{m_b^2}\,\overline{s}_\alpha \overleftarrow{D}_\rho(1+\gamma_5)D^\rho b_\alpha\,\overline{s}_\beta(1+\gamma_5)b_\beta \end{aligned} \qquad (23)$$

and the operators $\widetilde{R}_i$ which are obtained from the R_i's by interchanging the colour indices α and β of the two s fields [18]. At order $1/m_b$ only five of these operators are independent because of

relations like $\widetilde{R}_2 = -R_2 + \mathcal{O}(1/m_b^2)$. Writing (for $ab = cc, uc, uu$)

$$\widetilde{\Gamma}^{ab}_{12,1/m_b} \;=\; \frac{G_F^2 m_b^2}{24\pi M_{B_s}} \left[g_0^{ab} \langle B_s|R_0|\overline{B}_s\rangle \;+\; \sum_{j=1}^{3} \left[g_j^{ab} \langle B_s|R_j|\overline{B}_s\rangle + \widetilde{g}_j^{ab} \langle B_s|\widetilde{R}_j|\overline{B}_s\rangle \right] \right] \tag{24}$$

the coefficients g_j^{ab} and $\widetilde{g}_j^{ab}$ read [18, 21, 23]:

$$\begin{aligned}
g_0^{cc} \;&=\; \sqrt{1-4z}(1+2z)C_2^{(0)\,2} \;+\; F_S^{cc\,(0)} \;=\; \sqrt{1-4z}\,(1+2z)\,C_1^{(0)} \left[3C_1^{(0)} \;+\; 2\,C_2^{(0)}\right] \\
g_1^{cc} \;&=\; -2\sqrt{1-4z}(1+2z)\,C_1^{(0)} \left[3C_1^{(0)} \;+\; 2C_2^{(0)}\right] \qquad \widetilde{g}_1^{cc} \;=\; -2\sqrt{1-4z}(1+2z)C_2^{(0)\,2} \\
g_2^{cc} \;&=\; -2\,\frac{1-2z-2z^2}{\sqrt{1-4z}}\,C_1^{(0)} \left[3C_1^{(0)} \;+\; 2C_2^{(0)}\right] \qquad \widetilde{g}_2^{cc} \;=\; -2\,\frac{1-2z-2z^2}{\sqrt{1-4z}} C_2^{(0)\,2} \\
g_3^{cc} \;&=\; -24\,\frac{z^2}{\sqrt{1-4z}}\,C_1^{(0)} \left[3C_1^{(0)} \;+\; 2C_2^{(0)}\right] \qquad \widetilde{g}_3^{cc} \;=\; -24\,\frac{z^2}{\sqrt{1-4z}} C_2^{(0)\,2}
\end{aligned} \tag{25}$$

$$\begin{aligned}
g_0^{uc} \;&=\; (1-z)^2(1+2z)C_2^{(0)\,2} \;+\; F_S^{uc\,(0)} \;=\; (1-z)^2\,(1+2z)\,C_1^{(0)} \left[3C_1^{(0)} \;+\; 2\,C_2^{(0)}\right] \\
g_1^{uc} \;&=\; -2(1-z)^2(1+2z)\,C_1^{(0)} \left[3C_1^{(0)} \;+\; 2C_2^{(0)}\right] \qquad \widetilde{g}_1^{uc} \;=\; -2(1-z)^2(1+2z)C_2^{(0)\,2} \\
g_2^{uc} \;&=\; -2\,(1-z)\,(1+z+z^2)\,C_1^{(0)} \left[3C_1^{(0)} \;+\; 2C_2^{(0)}\right] \qquad \widetilde{g}_2^{uc} \;=\; -2\,(1-z)\,(1+z+z^2)C_2^{(0)\,2} \\
g_3^{uc} \;&=\; -12\,(1-z)\,z^2\,C_1^{(0)} \left[3C_1^{(0)} \;+\; 2C_2^{(0)}\right] \qquad \widetilde{g}_3^{uc} \;=\; -12\,(1-z)\,z^2\,C_2^{(0)\,2}.
\end{aligned} \tag{26}$$

and $g_j^{uu} = g_j^{cc}(z=0) = g_j^{uc}(z=0)$. Here

$$z \;\equiv\; \frac{\overline{m}_c^2}{\overline{m}_b^2} \;\equiv\; \frac{\left[\overline{m}_c(\overline{m}_c)\right]^2}{\left[\overline{m}_b(\overline{m}_b)\right]^2} \tag{27}$$

and $C_1^{(0)} \sim -0.3$ and $C_2^{(0)} \sim 1.1$ are the LO Wilson coefficients of the $\Delta B = 1$ operators Q_1 and Q_2 [16].

The contributions involving R_1, $\widetilde{R}_1$, R_3 and $\widetilde{R}_3$ are suppressed by powers of m_s/m_b or z^2 and are numerically negligible. The only two important $1/m_b$ operators are R_0 and $\widetilde{R}_2 = -R_2 + \mathcal{O}(1/m_b^2)$. As a consequence of the elimination of Q_S in favour of $\widetilde{Q}_S$ no term involving the large coefficient $C_2^{(0)\,2}$ occurs in g_0^{ab}. The contribution from R_0 is substantially diminished, and this can be understood in terms of a systematic expansion in $1/N_c$: the coefficients g_0^{ab} are colour–suppressed due to $C_1 \sim 1/N_c$, while they were colour–favoured in the old basis. Since radiative corrections cannot change the colour counting, this feature must persist in the yet uncalculated order α_s/m_b. In other words, by changing to our new basis we have absorbed the corrections of order N_c^0/m_b into the leading order of the $1/m_b$ expansion. This improves our result over the one in the old basis by a term of order $N_c\alpha_s/m_b$. (Recall that $\alpha_s \sim 1/N_c$, so that $N_c\alpha_s/m_b \sim N_c^0/m_b$.) This term (which constitutes a parametrically enhanced correction) would appear, if the calculation of α_s/m_b were done in the old basis. In fact, this term occurs in the NLO calculation of [19–21] in the coefficient of $\widetilde{Q}_S$ but is dropped once $\widetilde{Q}_S$ is traded for R_0, because all α_s/m_b

terms are consistently discarded. With the use of our new basis no corrections of order $N_c\alpha_s/m_b$ to g_0^{ab} can occur. This feature can also be understood by realising that the large–N_c contribution to Γ_{12}^{ab} stems from the right diagram in Fig. 2 with two insertions of Q_2 plus additional planar graphs with extra gluons. These diagrams contribute to the coefficients of Q and $\widetilde{Q}_S$, but not to the coefficient of Q_S. (This is easy to see, if one inserts the two Q_2's in the Fierz-rearranged form.) Upon elimination of Q_S in favour of R_0, the color–suppressed coefficient g^{ab} of Q_S becomes the coefficient of R_0. At order $1/m_b$ one has to include the momentum of the s quark in that diagram and finds a contribution to the $\widetilde{g}_i^{ab}$'s at order N_c^0. These terms are identical in both bases. Our numerical analysis in Sect. 3 follows the pattern revealed by the $1/N_c$ expansion, finding the numerical relevance of R_0 drastically reduced compared to the old basis, so that the only remaining important $1/m_b$ operator is $\widetilde{R}_2$.

In the new basis the $1/m_b$ corrections have their natural size of order $\overline{\Lambda}/m_b \sim 20\%$. To be conservative, we have estimated the $1/m_b^2$ terms to verify that this result is not accidental. We have found two types of contributions: the first type is calculated by expanding the results of Fig. 2 to the next order of the s–quark momentum, yielding operators with more derivatives acting on the s quark field. We find that these contributions have the same suppression pattern as the g_i^{ab}'s and $\widetilde{g}_i^{ab}$'s. The second type of $1/m_b^2$ operators involve the QCD field strength tensor $G_{\mu\nu}$ and has no counterparts at lower orders. We find small coefficients here as well. Since the size of the $1/m_b^2$ corrections is well below the uncertainty which we obtain by varying the bag factors of the operators in Eq. (23), there is no reason to include these corrections into our numerical code.

We parameterise the matrix elements $\langle R_i\rangle \equiv \langle B_s|R_i|\overline{B}_s\rangle$'s as

$$\begin{aligned}
\langle R_0\rangle &= -\frac{4}{3}\left[\frac{M_{B_s}^2}{m_b^{\rm pow\,2}\,(1+\overline{m}_s/\overline{m}_b)^2}-1\right] M_{B_s}^2 f_{B_s}^2 B_{R_0},\\
\langle R_1\rangle &= \frac{7}{3}\frac{\overline{m}_s}{\overline{m}_b} M_{B_s}^2 f_{B_s}^2 B_{R_1}, \qquad \langle \widetilde{R}_1\rangle = \frac{5}{3}\frac{\overline{m}_s}{\overline{m}_b} M_{B_s}^2 f_{B_s}^2 B_{\widetilde{R}_1},\\
\langle R_2\rangle &= -\frac{2}{3}\left[\frac{M_{B_s}^2}{m_b^{\rm pow\,2}}-1\right] M_{B_s}^2 f_{B_s}^2 B_{R_2}, \qquad \langle \widetilde{R}_2\rangle = \frac{2}{3}\left[\frac{M_{B_s}^2}{m_b^{\rm pow\,2}}-1\right] M_{B_s}^2 f_{B_s}^2 B_{\widetilde{R}_2},\\
\langle R_3\rangle &= \frac{7}{6}\left[\frac{M_{B_s}^2}{m_b^{\rm pow\,2}}-1\right] M_{B_s}^2 f_{B_s}^2 B_{R_3}, \qquad \langle \widetilde{R}_3\rangle = \frac{5}{6}\left[\frac{M_{B_s}^2}{m_b^{\rm pow\,2}}-1\right] M_{B_s}^2 f_{B_s}^2 B_{\widetilde{R}_3}. \qquad (28)
\end{aligned}$$

As usual the bag parameters $B_{R_0},\ldots,B_{\widetilde{R}_3}$ parameterise the deviation of the matrix elements from their VIA results derived in [18]. The numerical values of the $\langle R_i\rangle$'s depend sensitively on the choice of the mass parameter $m_b^{\rm pow}$ in Eq. (28). Clearly, $m_b^{\rm pow}$ is a redundant parameter, as any change in $m_b^{\rm pow}$ can be absorbed into the bag parameters. It merely serves to calibrate the overall size of the $1/m_b$-suppressed matrix elements such that the bag factors are close to 1. A future NLO calculation of the coefficients in Eq. (26) will allow us to replace $m_b^{\rm pow}$ by a well-defined (i.e. properly infrared-subtracted) b pole mass. Our numerical value for $m_b^{\rm pow}$ is guided by the requirement that the terms in square brackets in Eq. (28) are of order $2\overline{\Lambda}/m_b^{\rm pow} \sim 0.2$, which leads to the estimate $m_b^{\rm pow} \approx 4.8$ GeV. A better justification can be given by noting that the lattice computations of B, B_S and $\widetilde{B}_S$ in [22] allow for an estimate of $\langle R_0\rangle$ (which may

become a determination, once the lattice-continuum matching of $\langle R_0 \rangle$ is done at NLO):

$$B_{R_0} \;=\; \left[\frac{\alpha_1}{4}\widetilde{B}'_S + \alpha_2 B - \frac{5}{4}B'_S\right]\left[1 - \frac{M_{B_s}^2}{m_b^{\rm pow\,2}(1+\overline{m}_s/\overline{m}_b)^2}\right]^{-1} \tag{29}$$

With the central values for B, B_S and $\widetilde{B}_S$ given in [22] and the choice $m_b^{\rm pow} = 4.8$ GeV one finds $B_{R_0} = 1.1$, while those of the new preliminary lattice computation of [24] imply $B_{R_0} = 1.7$. Our quoted numerical results in Sect. 3 correspond to conservative ranges for both $m_b^{\rm pow}$ and the B_{R_i}'s. We note that the only places where we use $m_b^{\rm pow}$ are the matrix elements in Eq. (28); it is not used in the overall factor m_b^2 of $\widetilde{\Gamma}^{ab}_{12,1/m_b}$ in Eq. (24). This is a change compared to the analysis in [21].

2.3 Summing terms of order $\alpha_s^n z \ln^n z$

The coefficients G^{ab} and G_S^{ab} in Eq. (5) depend on quark masses through z defined in Eq. (27). At order α_s^n the dominant z-dependent terms are of the form $\alpha_s^n z \ln^n z$. In [25] and [21] it has been shown that these terms are summed to all orders $n = 1, 2, \ldots$, if one switches to a renormalisation scheme which uses

$$\overline{z} \;\equiv\; \frac{[\overline{m}_c(\overline{m}_b)]^2}{[\overline{m}_b(\overline{m}_b)]^2}. \tag{30}$$

Since $\overline{z}$ is roughly half as big as z, this also reduces the dependence of the coefficients on the charm mass. We illustrate the effect for Γ_{12}^{cc} with a numerical example: In the two renormalisation schemes one finds

$$\begin{aligned}
\Gamma_{12}^{cc} &= (3.3 \,-\, 11.4\,z \,+\, 1.5\,z\,\ln z)\cdot 10^{-3}\,\text{ps}^{-1} \,+\, \mathcal{O}\left(z^2\right) \\
\Gamma_{12}^{cc} &= (3.3 \,-\, 11.4\,\overline{z})\cdot 10^{-3}\,\text{ps}^{-1} \,+\, \mathcal{O}\left(\overline{z}^2\right).
\end{aligned} \tag{31}$$

The numerical input is taken from Eqs. (32–38) and Eq. (39) below. From Eq. (31) one verifies that the use of $\overline{z}$ eliminates the $z\ln z$ term. This issue is particularly relevant for $a_{\rm fs}^s$ and $a_{\rm fs}^d$, which are of order z. The final numbers for all quantities quoted below involve $\overline{z}$. We only revert to a scheme using z to compare with the previously published results in [19, 20].

3 Numerical predictions

3.1 Input

For the numerical analysis we use the following set of input parameters: The quark masses are [26]

$$\begin{aligned}
\overline{m}_b(\overline{m}_b) &= 4.22 \pm 0.08\,\text{GeV} \qquad \Rightarrow \quad m_b^{\rm pole} = 4.63 \pm 0.09\ \text{GeV} \\
m_b^{\rm pow} &= 4.8^{+0.0}_{-0.2}\,\text{GeV}
\end{aligned} \tag{32}$$

$$\begin{aligned} \overline{m}_c(\overline{m}_c) &= 1.30 \pm 0.05\,\mathrm{GeV} \;\Rightarrow\; z = \frac{\overline{m}_c^2(\overline{m}_c)}{\overline{m}_b^2(\overline{m}_b)} = 0.095 \pm 0.008\,, \\ &\Rightarrow\; \overline{z} = \frac{\overline{m}_c^2(\overline{m}_b)}{\overline{m}_b^2(\overline{m}_b)} = 0.048 \pm 0.004 \end{aligned} \tag{33}$$

$$\begin{aligned} \overline{m}_s(2\,\mathrm{GeV}) &= 0.10 \pm 0.02\,\mathrm{GeV} \quad\Rightarrow\quad \overline{m}_s(\overline{m}_b) = 0.085 \pm 0.017\,\mathrm{GeV} \\ m_t^{\mathrm{pole}} &= 171.4 \pm 2.1\,\mathrm{GeV} \quad\Rightarrow\quad \overline{m}_t(\overline{m}_t) = 163.8 \pm 2.0\,\mathrm{GeV} \end{aligned} \tag{34}$$

We will need the meson masses [27]

$$M_{B_d} = 5.279\,\mathrm{GeV}\,, \qquad M_{B_s} = 5.368\,\mathrm{GeV}\,. \tag{35}$$

The average width Γ_s of the B_s mass eigenstates is computed from the well-measured B_d lifetime,

$$\tau_{B_d} = 1.530 \pm 0.009\,\mathrm{ps}\,, \tag{36}$$

using $\Gamma_s = 1/\tau_{B_d}\,(1.00 \pm 0.01)$. Our input of the CKM elements is [2]

$$\begin{aligned} |V_{us}| &= 0.2248 \pm 0.0016\,, \qquad |V_{cb}| = (41.5 \pm 1.0) \cdot 10^{-3} \\ \left|\frac{V_{ub}}{V_{cb}}\right| &= 0.10 \pm 0.02\,, \qquad \gamma = 1.05^{+0.31}_{-0.12}\,. \end{aligned} \tag{37}$$

For all predictions within the standard model we assume unitarity of the CKM matrix and we determine all CKM elements from the four parameters $|V_{us}|$, $|V_{cb}|$, $|V_{ub}/V_{cb}|$ and γ. The W mass [27] and the strong coupling constant are [28]

$$M_W = 80.4\,\mathrm{GeV}\,, \qquad \alpha_s(M_Z) = 0.1189 \pm 0.0010\,. \tag{38}$$

We note that in the B_s system CKM parameters other than $|V_{cb}|$ (which basically determines $|V_{ts}|$) play a minor role. The same is true for the strange quark mass in Eq. (34).

The dominant theoretical uncertainties, however, stem from the non-perturbative parameters discussed below and from the dependence on the unphysical renormalisation scale μ_1. We use the central values $\mu_1 = \mu_2 = m_b$ and we vary μ_1 between $m_b/2$ and $2m_b$. The dependence on μ_2 is related to the determination of the hadronic quantities and uncertainties associated with μ_2 are contained in the quoted ranges for these quantities.

The situation of the non-perturbative parameters - the decay constant and the bag parameters - is not yet settled. Different non-perturbative methods result in quite different numerical results. QCD sum rule estimates were obtained for the decay constant f_{B_s} [29], for the bag parameter B [30, 31] and for B_S [31]. The same quantities have been determined in quenched approximation in numerous lattice simulations, see [32] for a review. The only determination of $\tilde{B}_S$ was done in a quenched lattice simulation in [22]. Unquenched ($n_f = 2$) values are available for f_{B_s} [33, 34], for B [34, 35] and for B_S [35, 36]. For the decay constant f_{B_s} even a lattice simulation with 2+1 dynamical fermions is available [37].

Unfortunately it turns out that the predictions for f_{B_s} vary over a wide range, $\mathcal{O}(200 \pm 20\,\mathrm{MeV})$ for quenched results, $\mathcal{O}(230 \pm 20\,\mathrm{MeV})$ for $n_f = 2$, $\mathcal{O}(245 \pm 20\,\mathrm{MeV})$ for sum rule estimates

and $\mathcal{O}(260 \pm 29\,\text{MeV})$ for $n_f = 2+1$, see e.g. [32]. This discrepancy has to be resolved, since ΔM and $\Delta\Gamma_s$ depend quadratically on the decay constant! Recently the combinations $f_{B_s}^2 B$, $f_{B_s}^2 B_S$ and $f_{B_s}^2 \tilde{B}_S$ were determined for 2+1 light flavors [24]. The authors of [24] claim that the combined determination results in a considerable reduction of the theoretical error.
We will use in our numerics two sets of non-perturbative parameters:
Set I consists of a conservative estimate for f_{B_s} combined with the unquenched determination for B [34] and B_S [36] and the only published lattice determination of $\tilde{B}_S$ [22]:

$$\begin{aligned} f_{B_s} &= 240 \pm 40\,\text{MeV} \\ B &= 0.85 \pm 0.06 \quad \Rightarrow \quad f_{B_s}\sqrt{B} = 0.221(46)\,\text{GeV} \\ B_S &= 0.86 \pm 0.08 \quad \Rightarrow \quad B'_S = 1.34 \pm 0.12 \quad \Rightarrow \quad f_{B_s}\sqrt{B'_S} = 0.277(57)\,\text{GeV} \\ \tilde{B}_S &= 0.91 \pm 0.08 \quad \Rightarrow \quad \tilde{B}'_S = 1.41 \pm 0.12 \quad \Rightarrow \quad f_{B_s}\sqrt{\tilde{B}'_S} = 0.285(60)\,\text{GeV} \end{aligned} \tag{39}$$

Set II consists of the preliminary determination with 2+1 flavors [24]:

$$\begin{aligned} f_{B_s}\sqrt{B} &= 0.227(17)\,\text{GeV} \\ f_{B_s}\sqrt{B'_S} &= 0.295(22)\,\text{GeV} \\ f_{B_s}\sqrt{\tilde{B}'_S} &= 0.305(23)\,\text{GeV} \end{aligned} \tag{40}$$

The central values of both sets are quite similar, while the errors of set II are smaller by almost a factor 3.
For both sets the bag parameters of the $1/m_b$-corrections are estimated within vacuum insertion approximation and we use the following conservative error estimate

$$B_{R_i} = 1 \pm 0.5\,. \tag{41}$$

In our computer programs we carefully extract all terms of order α_s^2 and α_s/m_b, which belong to yet uncalculated orders of the perturbation series, and discard them consistently.

3.2 ΔM_s within the SM

In the standard model expression (Eq.(2) & Eq.(4)) for the mass difference in the B_s-system a product of perturbative corrections ($\hat{\eta}_B S_0$) and non-perturbative corrections ($f_{B_s}^2 B$) arises. Using the above input the perturbative corrections are given by [9]

$$\hat{\eta}_B(\mu = \overline{m}_b) = 0.837\,(\text{NDR}), \tag{42}$$

$$S_0(x_t) = S_0\left(\frac{\overline{m}_t^2(\overline{m}_t)}{M_W^2}\right) = \frac{4x_t - 11x_t^2 + x_t^3}{4(1-x_t)^2} - \frac{3x_t^3\ln(x_t)}{2(1-x_t)^3} = 2.327 \pm 0.044 \tag{43}$$

Our final values for the standard model prediction

$$\Delta M_s = (19.30 \pm 6.68)\ \text{ps}^{-1} \quad \textbf{(Set I)} \tag{44}$$

$$\Delta M_s = (20.31 \pm 3.25)\ \text{ps}^{-1} \quad \textbf{(Set II)} \tag{45}$$

are bigger than the experimental result, but consistent within the errors. Using $f_{B_s} = 230$ MeV and the bag parameter from set I, one exactly reproduces the experimental value of ΔM_s.
The overall error is made up from the following components:

Input	ΔM_s Set I	ΔM_s Set II
f_{B_s}	$1^{+0.361}_{-0.306}$	$-$
B	1 ± 0.071	$-$
$f_{B_s}^2 B$	1 ± 0.341	1 ± 0.150
V_{cb}	$1^{+0.049}_{-0.048}$	$1^{+0.049}_{-0.048}$
$\alpha_s(M_Z)$	1 ± 0.020	1 ± 0.020
m_t	1 ± 0.018	1 ± 0.018
γ	$1^{+0.005}_{-0.015}$	$1^{+0.005}_{-0.015}$
$\lvert V_{ub}/V_{cb}\rvert$	1 ± 0.005	1 ± 0.005
$\sqrt{\sum \bar{\delta}^2}$	1 ± 0.346	1 ± 0.160

When combining different errors we first symmetrised the individual errors and added them quadratically afterwards. The by far dominant contribution to the error comes from the non-perturbative parameter $f_{B_s}^2 B$. Clearly, in view of the precise measurement in Eq. (7) it is highly desirable to understand the hadronic QCD effects with a much higher precision than today.

3.3 $\Delta\Gamma_s$, $\Delta\Gamma_s/\Delta M_s$ and $a_{\rm fs}^s$ within the SM

The main result of this paper is a new, more precise determination of Γ_{12}, which is then used to determine $\Delta\Gamma_s$, $\Delta\Gamma_s/\Delta M_s$ and $a_{\rm fs}^s$.

In order to illustrate our progress, we first present the results in the old operator basis used in [19,20]. Using the scheme involving $m_b^{\rm pole}$ and z as in [19,20], but updating the input parameters to our values in Eqs. (32–38), we find

$$\begin{aligned}
\Delta\Gamma_{s,old}^{\rm pole} &= \left(\frac{f_{B_s}}{240\,\text{MeV}}\right)^2 [0.002B + 0.094B'_S - \\
&\qquad \left(0.033B_{\tilde{R}_2} + 0.019B_{R_0} + 0.005B_R\right)] \text{ ps}^{-1} \\
\Delta\Gamma_{s,old}^{\rm pole,LO} &= \left(\frac{f_{B_s}}{240\,\text{MeV}}\right)^2 [0.005B + 0.145B'_S - \\
&\qquad \left(0.033B_{\tilde{R}_2} + 0.019B_{R_0} + 0.005B_R\right)] \text{ ps}^{-1} \\
a_{\rm fs,old}^{\rm pole,s} &= \left[10.8 + 1.9\frac{B'_S}{B} + 0.8\frac{B_R}{B}\right] \text{Im}\left(\frac{\lambda_u}{\lambda_t}\right) \cdot 10^{-4} \\
&+ \left[0.10 - 0.01\frac{B'_S}{B} + 0.29\frac{B_R}{B}\right] \text{Im}\left(\frac{\lambda_u}{\lambda_t}\right)^2 \cdot 10^{-4} \\
\left(\frac{\Delta\Gamma_s}{\Delta M_s}\right)_{old}^{\rm pole} &= \left[0.9 + 40.9\frac{B'_S}{B} - \left(14.4\frac{B_{\tilde{R}_2}}{B} + 8.5\frac{B_{R_0}}{B} + 2.1\frac{B_R}{B}\right)\right] \cdot 10^{-4}
\end{aligned} \tag{46}$$

For simplicity we do not show the uncertainties of the numerical coefficients appearing in the square brackets here and in following similar occasions. We assess these uncertainties, however, when quoting final results.

Several comments are in order: in the old basis the coefficient of B in the prediction of $\Delta\Gamma_s$ is negligible due to a cancellation among $\Delta B = 1$ Wilson coefficients, thus the term with B_S' dominates the overall result. This leads to the undesirable fact that the only coefficient in $\Delta\Gamma_s/\Delta M_s$ that is free from non-perturbative uncertainties is numerically negligible. Moreover in $\Delta\Gamma_s$ all $1/m_b$-corrections have the same size and add up to an unexpectedly large correction (30% of the LO value, 45% of the NLO value). In Eq. (46) we have singled out the bag factors of the two most important sub-dominant operators $\tilde{R}_2$ and R_0, while the bag parameters of the remaining operators are chosen equal and are denoted by B_R. Finally in the old operator basis the calculated NLO QCD corrections are large and reduce the final number by about 35% of the LO value.

$a_{\rm fs}^s$ does not suffer from this shortcomings. Here the coefficient without non-perturbative uncertainties is numerically dominant and the size of the $1/m_b$ corrections seems to be reasonable. Moreover in this case R_3 and $\tilde{R}_3$ are the dominant subleading operators. Since the overall contribution of the $1/m_b$-corrections is relatively small, we choose all bag factors of power suppressed operators equal to B_R.

Using the non-perturbative parameters from set I we obtain the following number for $\Delta\Gamma_s$:

$$\Delta\Gamma_s \;=\; (0.070 \pm 0.042)\ \text{ps}^{-1} \quad \Rightarrow \quad \frac{\Delta\Gamma_s}{\Gamma_s} = \Delta\Gamma_s \cdot \tau_{B_d} = 0.107 \pm 0.065 \tag{47}$$

This number is in agreement with previous estimates [19,38–40] where different input parameters - in particular different values for the decay constant and the bag parameters - were used. In the following table we quote the central values of these old predictions and in addition give the corresponding results adjusted to the new non-perturbative parameters of set I:

Reference	predicted $\Delta\Gamma_s/\Gamma_s$	used f_{B_s}	used B_S'	$\Delta\Gamma_s/\Gamma_s(f_{B_s} = 240\,\text{MeV}, B_S' = 1.34)$
[19]	0.054	210	1.02	0.117
[38]	0.093	230	1.25	0.114
[39]	0.124	245	1.36	0.116
[40]	0.118	245	1.31	0.117

The values in the last column are still bigger than the new number in Eq.(47) by about 8%. Besides some differences from other input parameters — like quark masses and CKM parameters — this small overestimate in the last column originates from the use of different methods to determine Γ_s in the ratio $\Delta\Gamma_s/\Gamma_s$ compared to this work. Since now very precise values of the b-lifetimes are available, we directly use them as an input to determine the total decay rate: $\Gamma_s = 1/\tau_{B_d}$. In [19, 38–40] we expressed the total decay rate in terms of the semileptonic decay rate: $\Gamma_s = \Gamma_{\rm sl}^{\rm theory}/B_{\rm sl}^{\rm exp}$. Doing so (with the 1998 value of $B_{\rm sl}^{\rm exp}$) one obtains values for $\tau_B \approx 1.66\,$ps, which are about 8% larger than the experimental number of $\tau_{B_d} \approx 1.53\,$ps.

The Rome group [20] used a different normalisation, guided by the wish to eliminate the huge

uncertainty due to f_{B_s}: $\Delta\Gamma_s/\Gamma_s = (\Delta\Gamma_s/\Delta M_s)^{\rm theory}(\Delta M_s/\Delta M_d)^{\rm theory}\Delta M_d^{\rm exp}\tau_{B_s}$. The values obtained by the Rome group for $\Delta\Gamma_s/\Gamma_s$ were typically considerably lower than 0.10, which was partially due to different input parameters like the bottom mass. Since now ΔM_s is known experimentally one can abbreviate their method to $\Delta\Gamma_s/\Gamma_s = (\Delta\Gamma_s/\Delta M_s)^{\rm theory}\Delta M_s^{\rm exp}\tau_{B_s}$. This prediction assumes that no new physics effects contribute to the mass difference. This is numerically equivalent to the use of $f_{B_s} = 230$ MeV in our approach (see the passage below Eq. (45)). With that input we obtain from our analysis $\Delta\Gamma_s/\Gamma_s = 0.10 \pm 0.06$ which is in perfect agreement with the latest update of the Rome group from this year [41]. Thus we see no discrepancy anymore between our predictions and those of the Rome group.

However, our predictions have been criticised recently in [12]. The authors of [12] obtain a much lower central value - $\Delta\Gamma_s/\Gamma_s = 0.067 \pm 0.027$ - and claim that this difference stems from their use of lattice values for the $1/m_b$-operators, while in our approach the vacuum insertion approximation was used. Lattice values for the $1/m_b$ corrections can be extracted from [22] for the operators R_0, R_1 and $\tilde{R}_1$, but their use does not resolve the numerical discrepancy. With the help of one author of [12] we have traced the difference back to the omission of the radiative corrections contained in α_1 and α_2, when Eq. (29) is used to extract $\langle R_0\rangle$ from lattice data on $\langle Q\rangle$, $\langle Q_S\rangle$ and $\langle\widetilde{Q}_S\rangle$. This is numerically equivalent to shifting B_{R_0} from 1.1 to 1.7. If we use this number and $f_{B_s} = 230$ MeV we obtain $\Delta\Gamma_s/\Gamma_s = 0.079$, which is closer to but still larger by 18% than the value obtained in [12].

Now we turn to the results in the new basis: For a direct comparison with the old operator basis, we first show results for the scheme characterised by $m_b^{\rm pole}$ and z:

$$\begin{aligned}
\Delta\Gamma_s^{\rm pole} &= \left(\frac{f_{B_s}}{240\,\text{MeV}}\right)^2 \Big[0.095B + 0.023\tilde{B}'_S - \\
&\qquad \Big(0.033B_{\tilde{R}_2} - 0.006B_{R_0} + 0.005B_R\Big)\Big]\ \text{ps}^{-1} \\
\Delta\Gamma_s^{\rm pole,LO} &= \left(\frac{f_{B_s}}{240\,\text{MeV}}\right)^2 \Big[0.121B + 0.029\tilde{B}'_S - \\
&\qquad \Big(0.033B_{\tilde{R}_2} - 0.006B_{R_0} + 0.005B_R\Big)\Big]\ \text{ps}^{-1} \\
a_{\rm fs}^{\rm pole,s} &= \left[12.9 + 0.5\frac{\tilde{B}'_S}{B} + 1.7\frac{B_R}{B}\right] \text{Im}\left(\frac{\lambda_u}{\lambda_t}\right)\cdot 10^{-4} \\
&+ \left[0.20 + 0.02\frac{\tilde{B}'_S}{B} + 0.44\frac{B_R}{B}\right] \text{Im}\left(\frac{\lambda_u}{\lambda_t}\right)^2\cdot 10^{-4} \qquad (48) \\
\left(\frac{\Delta\Gamma_s}{\Delta M_s}\right)^{\rm pole} &= \left[41.4 + 10.0\frac{\tilde{B}'_S}{B} - \left(14.4\frac{B_{\tilde{R}_2}}{B} - 2.6\frac{B_{R_0}}{B} + 2.1\frac{B_R}{B}\right)\right]\cdot 10^{-4} \qquad (49)
\end{aligned}$$

Now we are in the desired situation that $\Delta\Gamma_s$ is dominated by B and the lion's share of $\Delta\Gamma_s/\Delta M_s$ can be determined without any hadronic uncertainty! Moreover the size of the $1/m_b$-corrections has become smaller, because the magnitude of the contribution from R_0 is reduced by a factor of 3 (as anticipated from Eqs. (25) and (26)) and the sign of this contribution has changed. We are left with a $1/m_b$ correction of 22% of the LO value or 28% of the NLO-value. Using

the new operators the α_s-corrections have become smaller (22% of the LO value), too, and the unphysical μ_1-dependence has shrunk. In the case of $a_{\rm fs}^s = {\rm Im}\,(\Gamma_{12}^s/M_{12}^s)$ the situation did not change much due to the change of the basis. Here we have no strong recommendation on what basis to choose. However, in the presence of new physics $a_{\rm fs}^s$ also involves ${\rm Re}\,(\Gamma_{12}^s/M_{12}^s)$ and the same improvements occur, as discussed in Sect. 4.
Using the non-perturbative parameters from set I we obtain the following number for $\Delta\Gamma_s$:

$$\Delta\Gamma_s \;=\; (0.081 \pm 0.036)\ \text{ps}^{-1} \;\;\Rightarrow\;\; \frac{\Delta\Gamma_s}{\Gamma_s} = \Delta\Gamma_s \cdot \tau_{B_d} = 0.124 \pm 0.056 \tag{50}$$

The central value in the new basis is larger than the old one, while the theoretical errors have shrunk considerably. The numerical difference stems from uncalculated corrections of order α_s/m_b and α_s^2. As a consistency check of our change of basis one can compare the results in the old and the new basis neglecting all $1/m_b$ and α_s-corrections and setting $B = 1 = B'_S$. As required we get in both cases the same result: $\Delta\Gamma_s/\Gamma_s = 0.1497$.

For our final number we still go further. First we sum up logarithms of the form $z \ln z$ by switching to schemes using $\overline{z}$ defined in Eq. (30). Second we calculate our results for two schemes of the b-quark mass, using either $\overline{m}_b$ or $m_b^{\rm pole}$ of Eq. (32) and finally average over the schemes. By this we obtain the main result of this paper:

$$\begin{aligned}
\Delta\Gamma_s &= \left(\frac{f_{B_s}}{240\,\text{MeV}}\right)^2 \Big[(0.105 \pm 0.016)B + (0.024 \pm 0.004)\tilde{B}'_S \\
&\qquad - \Big((0.030 \pm 0.004)B_{\tilde{R}_2} - (0.006 \pm 0.001)B_{R_0} + 0.003 B_R\Big)\Big]\ \text{ps}^{-1} \qquad (51)\\
a_{\rm fs}^s &= \left[(9.7 \pm 1.6) + 0.3\frac{\tilde{B}'_S}{B} + 0.3\frac{B_R}{B}\right] \text{Im}\left(\frac{\lambda_u}{\lambda_t}\right) \cdot 10^{-4} \\
&+ \left[(0.08 \pm 0.01) + 0.02\frac{\tilde{B}'_S}{B} + (0.05 \pm 0.01)\frac{B_R}{B}\right] \text{Im}\left(\frac{\lambda_u}{\lambda_t}\right)^2 \cdot 10^{-4} \qquad (52)\\
\frac{\Delta\Gamma_s}{\Delta M_s} &= \left[(46.2 \pm 4.4) + (10.6 \pm 1.0)\frac{\tilde{B}'_S}{B}\right. \\
&\qquad \left. - \left((13.2 \pm 1.3)\frac{B_{\tilde{R}_2}}{B} - (2.5 \pm 0.2)\frac{B_{R_0}}{B} + (1.2 \pm 0.1)\frac{B_R}{B}\right)\right] \cdot 10^{-4} \qquad (53)
\end{aligned}$$

Using the parameter set I, we obtain the following final numbers

$$\begin{aligned}
\Delta\Gamma_s &= (0.096 \pm 0.039)\ \text{ps}^{-1} \;\;\Rightarrow\;\; \frac{\Delta\Gamma_s}{\Gamma_s} = \Delta\Gamma_s \cdot \tau_{B_d} = 0.147 \pm 0.060 && (54)\\
a_{\rm fs}^s &= (2.06 \pm 0.57) \cdot 10^{-5} && (55)\\
\frac{\Delta\Gamma_s}{\Delta M_s} &= (49.7 \pm 9.4) \cdot 10^{-4} && (56)\\
\phi_s &= (4.2 \pm 1.4) \cdot 10^{-3} \;=\; 0.24^\circ \pm 0.08^\circ && (57)
\end{aligned}$$

The first striking feature of these numbers is the large increase for the prediction of $\Delta\Gamma_s$ from 0.070 ps^{-1} to 0.096 ps^{-1} (about 37 %). The change of the basis is responsible for an increase of

about 16 $\%$. We have shown that the previously used basis suffers from several serious drawbacks — most importantly in the old basis strong cancellations, which are absent in the new basis, occur. Next we have reduced an additional uncertainty by summing up logarithms of the form $z \ln z$ to all orders. This theoretical improvement results in another increase of about 11%. The averaging over the pole and $\overline{\rm MS}$ schemes results in an increase of about 7% compared to the exclusive use of the pole-scheme. Finally we also include subleading CKM-structures (as done in [20, 21] as well) giving an increase of $\Delta\Gamma_s$ by about 3% compared to setting V_{ub} to zero. In the case of the flavour-specific CP-asymmetry the choice of the new basis has no dramatic effect. If one assumes that there is no new physics in the measured value of ΔM_s one can avoid the large uncertainty due to f_{B_s} by writing:

$$\Delta\Gamma_s = \left(\frac{\Delta\Gamma_s}{\Delta M_s}\right)^{\rm Theory} \cdot \Delta M_s^{\rm Exp.} = 0.088 \pm 0.017\,{\rm ps}^{-1} \tag{58}$$

$$\Rightarrow \quad \frac{\Delta\Gamma_s}{\Gamma_s} = \Delta\Gamma_s \cdot \tau_{B_d} = 0.127 \pm 0.024\,. \tag{59}$$

This smaller value is numerically equivalent to using $f_{B_s} = 230$ MeV in Eq. (51).
For completeness we also present the numbers with the parameter set II:

$$\Delta\Gamma_s = (0.106 \pm 0.032)\ {\rm ps}^{-1} \quad \Rightarrow \quad \frac{\Delta\Gamma_s}{\Gamma_s} = \Delta\Gamma_s \cdot \tau_{B_d} = 0.162 \pm 0.049 \tag{60}$$

$$a_{\rm fs}^s = (2.06 \pm 0.57) \cdot 10^{-5} \tag{61}$$

$$\frac{\Delta\Gamma_s}{\Delta M_s} = (51.9 \pm 9.8) \cdot 10^{-4} \tag{62}$$

The above errors in $\Delta\Gamma_s$ and ΔM_s have to be taken with some care, since we were not using our conservative error estimate but the preliminary values from [24].

In the following table the individual sources of uncertainties in $\Delta\Gamma_s$ — using the parameter set I — are listed in detail:

Input	$\Delta\Gamma_s$ old, pole, z	$\Delta\Gamma_s$ new, pole, z	$\Delta\Gamma_s$ new, average, $\overline{z}$
f_{B_s}	$1^{+0.361}_{-0.306}$	$1^{+0.361}_{-0.306}$	$1^{+0.361}_{-0.306}$
B_1	1 ± 0.002	$1^{+0.070}_{-0.071}$	1 ± 0.066
$B_{2,3}$	1 ± 0.167	1 ± 0.035	1 ± 0.031
$B_{\tilde{R}_2}$	1 ± 0.235	1 ± 0.203	1 ± 0.157
B_{R_0}	1 ± 0.140	1 ± 0.036	1 ± 0.030
μ_1 with $m_b/2 \leq \mu_1 \leq 2m_b$	$1^{+0.248}_{-0.521}$	$1^{+0.111}_{-0.272}$	$1^{+0.074}_{-0.200}$
V_{cb}	$1^{+0.049}_{-0.048}$	$1^{+0.049}_{-0.048}$	1 ± 0.049
z	$1^{+0.044}_{-0.046}$	$1^{+0.040}_{-0.042}$	1 ± 0.019
m_b	$1^{+0.043}_{-0.042}$	$1^{+0.036}_{-0.035}$	$1^{+0.010}_{-0.009}$
α_s	$1^{+0.014}_{-0.013}$	1 ± 0.003	1 ± 0.001
m_s	1 ± 0.010	1 ± 0.012	1 ± 0.010
γ	$1^{+0.005}_{-0.016}$	$1^{+0.005}_{-0.015}$	$1^{+0.005}_{-0.014}$
$\lvert V_{ub}/V_{cb}\rvert$	1 ± 0.006	1 ± 0.006	1 ± 0.005
$\sqrt{\sum \bar{\delta}^2}$	1 ± 0.607	1 ± 0.450	1 ± 0.405
$m_b^{\rm pow}$	$1_{-0.368}$	$1_{-0.158}$	$1_{-0.112}$
RS	1 ± 0.133	1 ± 0.065	1 ± 0.066

(63)

The same result is visualised in figure 3. In the case of $\Delta\Gamma_s$ the by far largest uncertainty stems from the error on f_{B_s}. Here a considerable improvement from the non-perturbative side is mandatory. The dependence on the decay constant is of course not affected by the change of the operator basis. The second most important uncertainty comes from the $1/m_b$-operator $\tilde{R}_2$. This operator has up to now only been estimated in the naive vacuum insertion approximation. Any non-perturbative investigation would be very helpful. Number three in the error hit list is the unphysical μ_1-dependence. Using the old operator basis the corresponding error was huge, it was drastically reduced by changing to the new basis and by including also the $\overline{\rm MS}$-scheme for the b-quark mass. Any further improvement requires a cumbersome NNLO calculation, which might be worthwhile if progress on the non-perturbative side for f_{B_s} and $\tilde{R}_2$ is achieved. Number four is again a non-perturbative parameter - now the bag parameter of the operator Q. In the old operator basis the corresponding uncertainty stemmed from B_S and was larger by a factor of 2.5. The dependence on V_{cb} results in a relative error of about 5% for both the old basis and the new basis. All remaining uncertainties are at most 3%.

Using our conservative estimates and adding all errors quadratically (after symmetrising them) we arrive at a reduction of the overall theoretical error due to the introduction of the new basis from $\pm 61\%$ to $\pm 41\%$, where the last number is completely dominated by the decay constant. If one neglects the dependence on f_{B_s} the overall theoretical error goes down from $\pm 51\%$ to $\pm 23\%$.

In the table in Eq. (63) we also show the dependence on the b-quark mass we are using in the $1/m_b$-corrections, $m_b^{\rm pow}$. This dependence can be viewed as a measure of the overall size of the

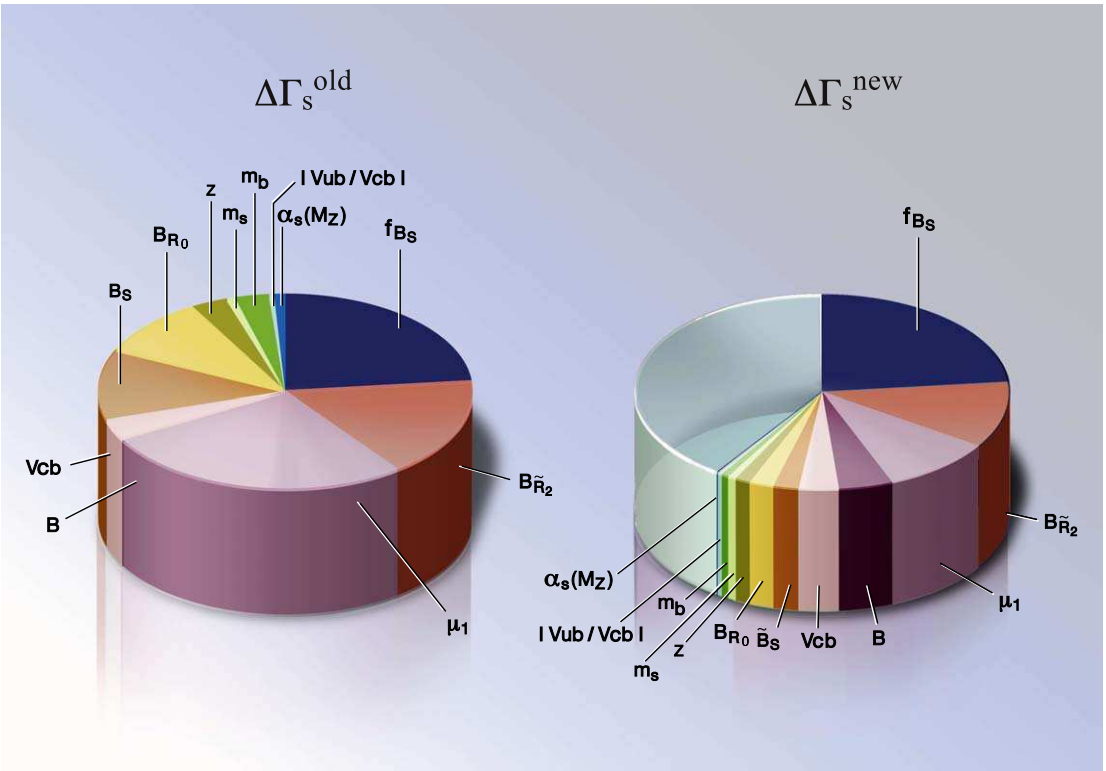

Figure 3: Uncertainty budget for the theory prediction of $\Delta\Gamma_s$. The largest uncertainties stem from f_{B_s}, the renormalisation scale μ_1 of the $\Delta B = 1$ operators and the bag parameter of the $1/m_b$–suppressed operator $\tilde{R}_2$. The transparent segment of the right pie chart shows the improvement with respect to the old result on the left.

$1/m_b$-corrections. The use of the new basis results in a strong reduction of the corresponding uncertainty, from 37% to 11%. And finally we compare the two renormalisation schemes (RS) we are using for the b-quark mass. Here we have again muss less uncertainty in the new operator basis. To avoid a double counting of the errors we did not include the last two rows of table (63) in the total error.

Investigating the case of $\Delta\Gamma_s/\Delta M_s$ the improvement due to our new basis is more substantial, since here the dependence on f_{B_s} cancels:

Input	$\Delta\Gamma_s/\Delta M_s$ old, pole, z	$\Delta\Gamma_s/\Delta M_s$ new, average, $\overline{z}$	$a^s_{\rm fs}$ new, average, $\overline{z}$
B_1	$1^{+0.074}_{-0.064}$	1 ± 0.005	$1^{+0.006}_{-0.005}$
$B_{2,3}$	1 ± 0.167	1 ± 0.031	1 ± 0.004
$B_{\tilde{R}_2}$	1 ± 0.235	1 ± 0.157	$1 \pm 0.025(\tilde{R}_3)$
B_{R_0}	1 ± 0.140	1 ± 0.030	$1 \pm 0.011(R_3)$
μ_1 with $m_b/2 \le \mu_1 \le 2m_b$	$1^{+0.194}_{-0.495}$	$1^{+0.027}_{-0.154}$	$1^{+0.152}_{-0.101}$
V_{cb}	1 ± 0.000	1 ± 0.000	1 ± 0.000
z	$1^{+0.044}_{-0.046}$	1 ± 0.019	$1^{+0.094}_{-0.092}$
m_b	$1^{+0.043}_{-0.042}$	$1^{+0.010}_{-0.009}$	$1^{+0.037}_{-0.036}$
m_t	1 ± 0.018	1 ± 0.018	1 ± 0.018
α_s	1 ± 0.012	1 ± 0.001	1 ± 0.007
m_s	1 ± 0.010	1 ± 0.010	1 ± 0.001
γ	$1^{+0.001}_{-0.003}$	$1^{+0.000}_{-0.001}$	$1^{+0.144}_{-0.081}$
$\lvert V_{ub}/V_{cb}\rvert$	1 ± 0.001	1 ± 0.001	$1^{+0.194}_{-0.196}$
$\sqrt{\sum \bar{\delta}^2}$	1 ± 0.480	1 ± 0.189	1 ± 0.279
$m_b^{\rm pow}$	$1_{-0.368}$	$1_{-0.112}$	$1^{+0.016}$
RS	1 ± 0.136	1 ± 0.069	1 ± 0.004

In the case of $\Delta\Gamma_s/\Delta M_s$ the use of the new operator basis leads to a reduction of the total error from 48% to 19%! The dominant error is now due to the bag parameter $B_{\tilde{R}_2}$, followed by the μ_1-dependence. The remaining uncertainties are at most 3%. In the case of $a^s_{\rm fs}$ the situation is quite different. Here the dominant uncertainty stems from V_{ub}, followed by the dependences on μ_1, γ and $\overline{z}$. Moreover the $1/m_b$-corrections play a minor role here — as can be read off from the error due to the variation of $m_b^{\rm pow}$.

3.4 ΔM_d, $\Delta\Gamma_d$ and $a^d_{\rm fs}$ within the SM

Here we give updated numbers for the mixing parameters of the B_d system. The CKM elements governing $B_d - \overline{B}_d$ mixing appear in the combinations $\lambda^d_i = V^*_{id}V_{ib}$ for $i = u, c, t$. The bag parameters multiplying f_{B_d} below refer to B_d mesons and are different from those in the B_s system. However, no non-perturbative computation has shown any numerically relevant deviation of B_{B_d}/B_{B_s} from 1.

Updating ΔM_d to $\overline{m}_t(\overline{m}_t) = 163.8 \pm 2.0\,\text{GeV}$ gives

$$\Delta M_d = (0.53 \pm 0.02)\,\text{ps}^{-1}\left(\frac{|V_{td}|}{0.0082}\right)^2 \left(\frac{f_{B_d}}{200\,\text{MeV}}\right)^2 \frac{B}{0.85}.$$

While in the B_s system the values of γ and $|V_{ub}|$ in Eq. (37) play a minor role, their uncertainties are an issue for $\Delta\Gamma_d$ and $a^d_{\rm fs}$. The master formulae are [21]

$$\frac{\Delta\Gamma_d}{\Delta M_d} \;=\; -10^{-4}\left[c \;+\; a\,\text{Re}\,\frac{\lambda^d_u}{\lambda^d_t} \;+\; b\,\text{Re}\,\frac{\lambda^{d\,2}_u}{\lambda^{d\,2}_t}\right] \tag{64}$$

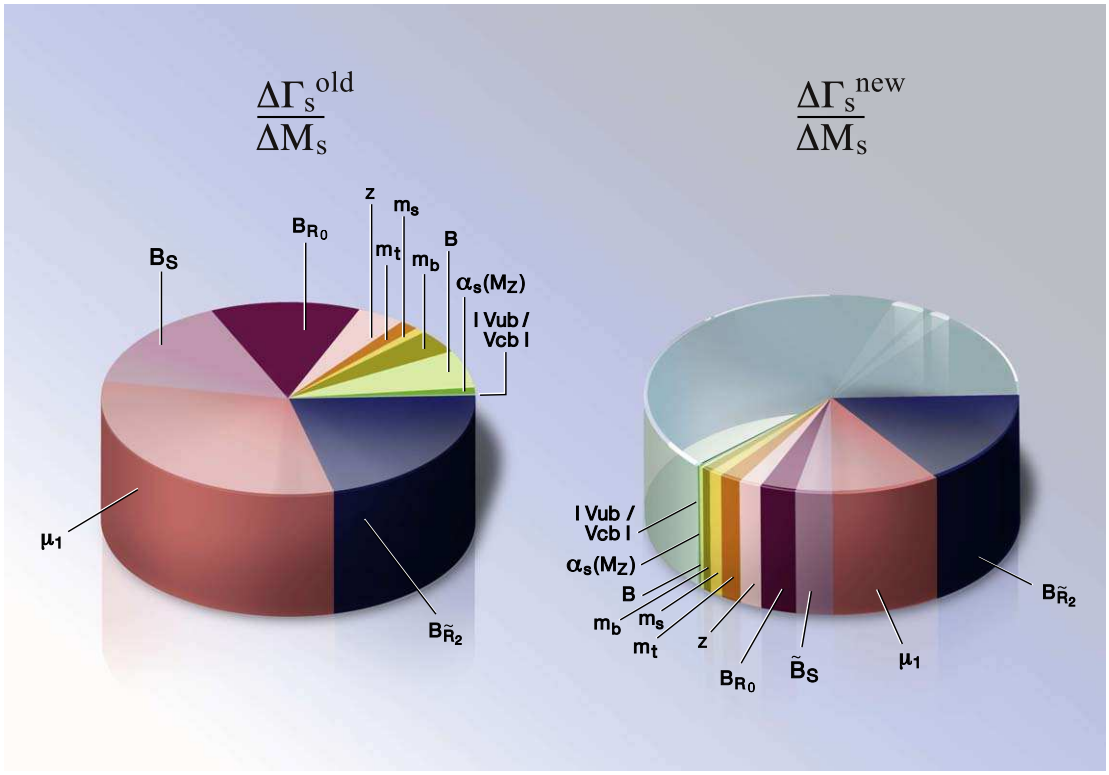

Figure 4: Uncertainty budget for $\Delta\Gamma_s/\Delta M_s$. See Fig. 3 for explanations. The ratio $\Delta\Gamma_s/\Delta M_s$ does not depend on f_{B_s} and the progress due to the new operator basis is more substantial than in $\Delta\Gamma_s$.

$$a_{\rm fs}^d \;=\; 10^{-4}\left[a\,{\rm Im}\,\frac{\lambda_u^d}{\lambda_t^d} \;+\; b\,{\rm Im}\,\frac{\lambda_u^{d\,2}}{\lambda_t^{d\,2}}\right]. \tag{65}$$

The coefficients

$$\begin{aligned} a \;&=\; 2\cdot 10^4\,\frac{\Gamma_{12}^{uc}-\Gamma_{12}^{cc}}{M_{12}^d/\lambda_t^{d\,2}}, \qquad b \;=\; 10^4\,\frac{2\Gamma_{12}^{uc}-\Gamma_{12}^{cc}-\Gamma_{12}^{uu}}{M_{12}^d/\lambda_t^{d\,2}} \\ \text{and} \quad c \;&=\; -10^4\,\frac{\Gamma_{12}^{cc}}{M_{12}^d/\lambda_t^{d\,2}} \end{aligned} \tag{66}$$

are independent of CKM elements because of $M_{12}^d \propto \lambda_t^{d\,2}$. In our new operator basis these coefficients read

$$\begin{aligned} a \;&=\; 9.68^{+1.53}_{-1.48} \;+\; \left(0.31^{+0.09}_{-0.07}\right)\frac{\widetilde{B}'_S}{B} \;+\; \left(0.27^{+0.15}_{-0.06}\right)\frac{B_R}{B} \\ b \;&=\; 0.08\pm 0.03 \;+\; (0.02\pm 0.01)\,\frac{\widetilde{B}'_S}{B} \;+\; \left(0.04^{+0.03}_{-0.01}\right)\frac{B_R}{B} \\ c \;&=\; -46.1\pm 6.6 \;-\; (10.5\pm 1.3)\,\frac{\widetilde{B}'_S}{B} \;+\; \left(8.7^{+4.9}_{-1.0}\right)\frac{B_R}{B}. \end{aligned}$$

With the hadronic parameters of Set I in Eq. (39) one finds

$$a \;=\; 10.5^{+1.8}_{-1.7}, \qquad b \;=\; 0.2 \pm 0.1, \qquad c \;=\; -53.3^{+12.7}_{-11.4} \tag{67}$$

It is convenient to express λ_u^d/λ_t^d in Eqs. (64) and (65) in terms of the angle $\beta = \arg(-\lambda_t^d/\lambda_c^d)$ of the unitarity triangle and the length $R_t = |\lambda_t^d/\lambda_c^d|$ of the adjacent side [21]:

$$\begin{aligned} \mathrm{Re}\,\frac{\lambda_u^d}{\lambda_t^d} &= \frac{\cos\beta}{R_t} - 1, \qquad \mathrm{Re}\,\frac{\lambda_u^{d\,2}}{\lambda_t^{d\,2}} \;=\; \frac{\cos(2\beta)}{R_t^2} - 2\frac{\cos\beta}{R_t} + 1, \\ \mathrm{Im}\,\frac{\lambda_u^d}{\lambda_t^d} &= -\frac{\sin\beta}{R_t}, \qquad \mathrm{Im}\,\frac{\lambda_u^{d\,2}}{\lambda_t^{d\,2}} \;=\; -\frac{\sin(2\beta)}{R_t^2} + 2\frac{\sin\beta}{R_t}. \end{aligned} \tag{68}$$

Clearly the terms involving $\lambda_u^{d\,2}/\lambda_t^{d\,2}$ in Eqs. (64) and (65) are numerically irrelevant in view of the smallness of b. Moreover, in the preferred region of the Standard Model fit of the unitarity triangle one has $\cos\beta \approx R_t$, so that $\mathrm{Re}\,\lambda_u^d/\lambda_t^d$ is suppressed. Setting a and b to zero in Eq. (64) reproduces $\Delta\Gamma_d/\Delta M_d$ within 2% [21] and $\Delta\Gamma_d/\Delta M_d$ is essentially free of CKM uncertainties.

Inserting Eqs. (67) and (68) into Eqs. (64) and (65) yields

$$\begin{aligned} \frac{\Delta\Gamma_d}{\Delta M_d} \;=\; \Bigg[& 53.3^{+11.4}_{-12.7} \;+\; \left(10.3^{+1.8}_{-1.7}\right)\left(1 \;-\; \frac{\cos(\beta)}{R_t}\right) \\ & + (0.2 \pm 0.1)\left(\frac{\cos(\beta)}{R_t} - \frac{\cos(2\beta)}{R_t^2}\right)\Bigg] \cdot 10^{-4} \end{aligned} \tag{69}$$

$$a_{\rm fs}^d \;=\; -\left[\left(10.1^{+1.8}_{-1.7}\right)\frac{\sin\beta}{R_t} \;+\; (0.2 \pm 0.1)\,\frac{\sin(2\beta)}{R_t^2}\right] \cdot 10^{-4} \tag{70}$$

Next we insert the numerical values for β and R_t from [2]. Since we are interested in testing the hypothesis of new physics in $B_s - \overline{B}_s$ mixing, we take values for β and R_t obtained prior to the measurement of ΔM_s. With $\beta = 23^\circ \pm 2^\circ$ and $R_t = 0.86 \pm 0.11$, which correspond to a CL of 2σ, one finds

$$\frac{\Delta\Gamma_d}{\Delta M_d} \;=\; \left(52.6^{+11.5}_{-12.8}\right) \cdot 10^{-4}, \qquad\qquad a_{\rm fs}^d \;=\; \left(-4.8^{+1.0}_{-1.2}\right) \cdot 10^{-4}. \tag{71}$$

Thus these predictions allow for new physics in ΔM_s, but assume that all other quantities entering the standard fit of the unitarity triangle in [2] are as in the Standard Model. Using $\Delta M_d^{\rm exp} = 0.507 \pm 0.004\,\mathrm{ps}^{-1}$ and $\tau_{B_d}^{\rm exp} = 1.530 \pm 0.009$ we find from Eq. (71):

$$\Delta\Gamma_d \;=\; \frac{\Delta\Gamma_d}{\Delta M_d}\,\Delta M_d^{\rm exp} \;=\; \left(26.7^{+5.8}_{-6.5}\right) \cdot 10^{-4}\,\mathrm{ps}^{-1}, \qquad \frac{\Delta\Gamma_d}{\Gamma_d} \;=\; \left(40.9^{+8.9}_{-9.9}\right) \cdot 10^{-4}. \tag{72}$$

The result in Eq. (72) is consistent with our prediction in [21], but the central value is substantially higher. This is not solely caused by our new operator basis, but also by the use of a different renormalisation scheme. In both [21] and this work we average over two schemes, but in one

of the schemes used in [21] the $z \ln z$ terms are not summed to all orders. Note that the quoted error of $a_{\rm fs}^d$ in [21] corresponds to the 1σ ranges of β and R_t, while in Eq. (71) more conservative 2σ intervals have been used. The ranges in Eq. (71) imply for the CP-violating phase $\phi_d = \arg(-M_{12}^d/\Gamma_{12}^d)$:

$$\phi_d \;=\; -0.091^{+0.026}_{-0.038} \;=\; -5.2^{\circ\,+1.5^\circ}_{-2.1^\circ}\,. \tag{73}$$

4 Constraining new physics with $B_s - \overline{B}_s$ mixing

In this section we investigate effects of new physics contributions to the B_s-mixing parameters. New physics can change the magnitude and the phase of M_{12}^s. We parameterise its effect (similarly to [2, 42]) by

$$M_{12}^s \;\equiv\; M_{12}^{\rm SM,s}\cdot\Delta_s\,, \qquad\qquad \Delta_s \;\equiv\; |\Delta_s| e^{i\phi_s^\Delta}. \tag{74}$$

The relationship to the parameters used in [2, 14] is

$$\Delta_s \;=\; r_s^2 e^{2i\theta_s}.$$

We find it more transparent to plot $\mathrm{Im}\,\Delta_s$ vs. $\mathrm{Re}\,\Delta_s$ than to plot $2\theta_s$ vs. r_s^2. Our plots are similar to Fig. 1 of [14], which displays $\sin(2\theta_s)$ vs. $\cos(2\theta_s)$, but also include the information on $|\Delta_s| \equiv r_s^2$. Finally Γ_{12}^s stems from CKM-favoured tree decays and one can safely set $\Gamma_{12}^s = \Gamma_{12}^{\rm SM,s}$.

4.1 $\Delta\Gamma_s$, $\Delta\Gamma_s/\Delta M_s$ and $a_{\rm fs}^s$ beyond the SM

One easily finds:

$$\Delta M_s \;=\; \Delta M_s^{\rm SM}\,|\Delta_s| = (19.30 \pm 6.74)\,\text{ps}^{-1}\cdot|\Delta_s| \tag{75}$$

$$\Delta\Gamma_s \;=\; 2|\Gamma_{12}^s|\,\cos\left(\phi_s^{\rm SM}+\phi_s^\Delta\right) = (0.096\pm 0.039)\,\text{ps}^{-1}\cdot\cos\left(\phi_s^{\rm SM}+\phi_s^\Delta\right) \tag{76}$$

$$\frac{\Delta\Gamma_s}{\Delta M_s} \;=\; \frac{|\Gamma_{12}^s|}{|M_{12}^{\rm SM,s}|}\cdot\frac{\cos\left(\phi_s^{\rm SM}+\phi_s^\Delta\right)}{|\Delta_s|} = (4.97\pm 0.94)\cdot 10^{-3}\cdot\frac{\cos\left(\phi_s^{\rm SM}+\phi_s^\Delta\right)}{|\Delta_s|} \tag{77}$$

$$a_{\rm fs}^s \;=\; \frac{|\Gamma_{12}^s|}{|M_{12}^{\rm SM,s}|}\cdot\frac{\sin\left(\phi_s^{\rm SM}+\phi_s^\Delta\right)}{|\Delta_s|} = (4.97\pm 0.94)\cdot 10^{-3}\cdot\frac{\sin\left(\phi_s^{\rm SM}+\phi_s^\Delta\right)}{|\Delta_s|} \tag{78}$$

$$\text{with (cf. Eq. (57))} \qquad \phi_s^{\rm SM} = (4.2\pm 1.4)\cdot 10^{-3} \tag{79}$$

Here the numerical values correspond to our results from parameter set I in Eqs. (54–57). In the case of $a_{\rm fs}^s$ there is a major difference to the SM case of Sect. 3.3, which only involves $\mathrm{Im}\,(\Gamma_{12}^s/M_{12}^s)$: in the presence of new physics $a_{\rm fs}^s$ is dominated by $\mathrm{Re}\,(\Gamma_{12}^s/M_{12}^s)$ as long as $|\phi_s^\Delta| > \phi_s^{\rm SM}$. Thus the prediction in Eq. (78) profits from the improvements due to our new operator basis — just as the prediction of $\Delta\Gamma_s$ in Eq. (77). From Eq. (78) one also verifies the enormous sensitivity of $a_{\rm fs}^s$ to new physics, since it exceeds its SM value by a factor of 250 for $\phi_s^\Delta = \pi/2$. We have plotted $a_{\rm fs}^s$ vs. ϕ_s^Δ for the old and the new bases in Fig. 5.

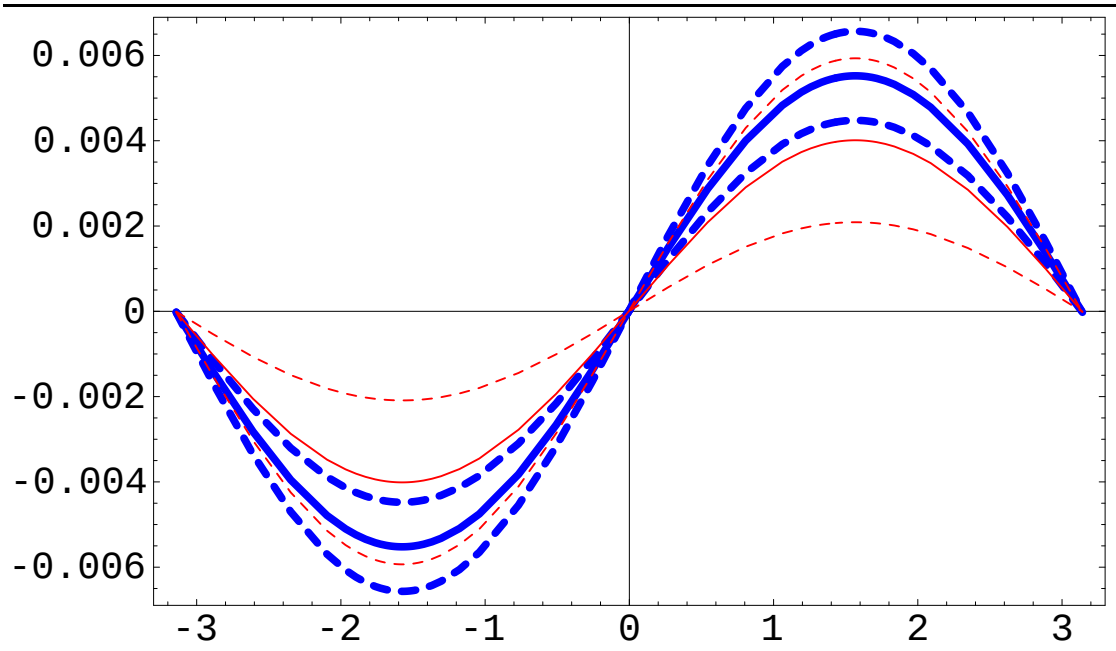

Figure 5: $a^s_{\rm fs}$ as a function of the new phase ϕ_s^Δ from Eq. (78) for the range $-\pi \le \phi_s^\Delta \le \pi$. The thick blue lines show the prediction in the new basis, while thin red lines correspond to the old operator basis. The solid lines display the central values of our predictions and the dashed lines show the uncertainties, which are much larger for the old result. The standard model value $a^s_{\rm fs}(\phi_s^\Delta = 0) = 2.1 \cdot 10^{-5}$ is too close to zero to be visible in the plot.

4.2 Basic observables

In this section we summarise the observables which constrain $|\Delta_s|$ and ϕ_s^Δ. These constraints are illustrated in Fig. 6 for hypothetical measurements.

1. The mass difference ΔM_s determines $|\Delta_s|$ through Eq. (75). The accuracy of $|\Delta_s|$ extracted from ΔM_s is limited by the precision of a lattice computation. This is not the case for the other quantities discussed in this section.

Alternatively one can confront the experimental ratio $\Delta M_d/\Delta M_s$ with theory. This has the advantage that the ratio of the hadronic matrix elements involved can be predicted with a smaller error, of order 5%. However, then the parameter of R_t of the unitarity triangle entering ΔM_d must be taken from measurements which are insensitive to new physics (or at least insensitive to new physics in $B_s - \overline{B}_s$ mixing), e.g. through determinations of the CKM angle γ from tree-level B decays (cf. the discussion after Eq. (70)). At present this method leads to comparable uncertainties in the extracted $|\Delta_s|$ as the direct determination from ΔM_s. (Further flavour-blind new physics cancels from $\Delta M_d/\Delta M_s$.) In the following analyses we do not use $\Delta M_d/\Delta M_s$.

2. The lifetime measurement in an untagged $b \to c\overline{c}s$ decay $\overline{(B}_s) \to f_{CP}$, where f_{CP} is a CP eigenstate, determines $\Delta\Gamma_s \cos(\phi_s^\Delta - 2\beta_s) = |\Delta\Gamma_s \cos(\phi_s^\Delta - 2\beta_s)|$ [43, 44]. Consider a CP-even

final state f_{CP+} like $D_s^+ D_s^-$. The time-dependent decay rate reads

$$\begin{aligned}\Gamma[{}^{(}\overline{B}_s^{)} \to f_{CP+}, t] &\propto \frac{1+\cos(\phi_s^\Delta - 2\beta_s)}{2} e^{-\Gamma_L t} \;+\; \frac{1-\cos(\phi_s^\Delta - 2\beta_s)}{2} e^{-\Gamma_H t} \\ &= \; e^{-\Gamma_s t}\left[\cosh\frac{\Delta\Gamma_s\, t}{2} - \cos(\phi_s^\Delta - 2\beta_s)\sinh\frac{\Delta\Gamma_s\, t}{2}\right] \end{aligned} \tag{80}$$

and the (time-independent) overall normalisation is related to the branching fraction [44]. Here

$$\beta_s \;=\; -\arg\left(-\frac{\lambda_t^s}{\lambda_c^s}\right) \;=\; 0.020 \pm 0.005 \;=\; 1.1^\circ \pm 0.3^\circ. \tag{81}$$

That is, $-\beta_s$ is the analogue of the angle β of the unitarity triangle, which governs the mixing-induced CP asymmetry in $B_d \to J/\psi K_S$, in the B_s system. For β_s different sign conventions are used in the literature, we chose the one of [6] which satisfies $\beta_s > 0$.

For example within the Standard Model (and neglecting the tiny β_s) the lifetime measured in ${}^{(}\overline{B}_s^{)} \to D_s^+ D_s^-$ equals $\Gamma_L^s = \Gamma_s + \Delta\Gamma/2$, because only the short-lived CP-even mass eigenstate B_L can decay into $D_s^+ D_s^-$. By using the theory relation $1/\tau_{B_d} = \Gamma_d = (1.00 \pm 0.01)\Gamma_s$ one then finds $\Delta\Gamma_s$. For $\phi_s^\Delta \neq 0$, however, the mass eigenstates are no more CP eigenstates and both of them can decay to a CP eigenstate, as can be easily verified from Eq. (80). From $\Gamma[{}^{(}\overline{B}_s^{)} \to f_{CP+}, t]$ one can extract $|\Gamma_s|$, $|\Delta\Gamma_s|$, $|\cos(\phi_s^\Delta)|$ and the overall normalisation, if the statistics is high enough to separate the two exponentials. If the measured $\Gamma[{}^{(}\overline{B}_s^{)} \to f_{CP+}, t]$ is fitted to a single exponential $\exp[-\Gamma_f\, t]$, the measured rate is [44, 45]

$$\Gamma_f \;=\; \frac{(1+\cos(\phi_s^\Delta - 2\beta_s))/\Gamma_L + (1-\cos(\phi_s^\Delta - 2\beta_s))/\Gamma_H}{(1+\cos(\phi_s^\Delta - 2\beta_s))/\Gamma_L^2 + (1-\cos(\phi_s^\Delta - 2\beta_s))/\Gamma_H^2} \tag{82}$$

$$\begin{aligned} &= \; \Gamma_s \;+\; \Delta\Gamma_s \cos(\phi_s^\Delta - 2\beta_s) \;+\; \mathcal{O}\left(\frac{(\Delta\Gamma_s)^2}{\Gamma_s}\right) \\ &= \; \Gamma_s \;+\; 2\,|\Gamma_{12}^s| \cos(\phi_s^\Delta + \phi_s^{\rm SM}) \cos(\phi_s^\Delta - 2\beta_s) \;+\; \mathcal{O}\left(\frac{(\Delta\Gamma_s)^2}{\Gamma_s}\right). \end{aligned} \tag{83}$$

For a CP-odd final state one has to interchange Γ_L and Γ_H in Eqs. (80) and (82) and to flip the sign of $\cos(\phi_s^\Delta - 2\beta_s)$ in Eqs. (80) and (83). From Eq. (83) it is clear that the lifetime measurement determines [43, 44]

$$\Delta\Gamma_s \cos(\phi_s^\Delta) \;=\; 2|\Gamma_{12}^s| \cos^2(\phi_s^\Delta),$$

if the small phases $\phi_s^{\rm SM}$ and β_s are neglected. Thus one can find $|\cos\phi_s^\Delta|$, which determines ϕ_s^Δ with a four-fold ambiguity.* We stress that (since sign $\Delta\Gamma_s =$ sign $\cos(\phi_s^\Delta)$) the lifetime method gives no information on the sign of $\Delta\Gamma_s$ and experimental results should be quoted for $|\Delta\Gamma_s|$ rather than $\Delta\Gamma_s$.

*If one keeps $\phi_s^{\rm SM}$ and β_s non-zero, one solution for ϕ_s^Δ is related to the other three by $\phi_s^\Delta \to \phi_s^\Delta + \pi$, $\phi_s^\Delta \to 2\beta_s - \phi_s^{\rm SM} - \phi_s^\Delta$ and $\phi_s^\Delta \to 2\beta_s - \phi_s^{\rm SM} - \phi_s^\Delta + \pi$.

Eq. (82) assumes that detection efficiencies are constant over the decay time. Since this is not the case in real experiments, we strongly recommend to perform a three-parameter fit to $2|\Gamma_{12}|$, $|\cos(\phi_s^\Delta)|$ and the overall normalisation (with $|\Gamma_s|$ fixed to $|\Gamma_d|(1.00 \pm 0.01)$) to Eq. (80).

With the advent of the precise measurement of ΔM_s [10] one will rather exploit $|\Delta\Gamma_s|/\Delta M_s$ to constrain Δ_s than $|\Delta\Gamma_s|$ itself, which suffers from much larger hadronic uncertainties. From Eq. (77) one infers that $|\Delta\Gamma_s|/\Delta M_s$ defines two circles in the complex Δ_s plane which touch the y–axis at the origin.

3. The angular analysis of an untagged $b \to c\overline{c}s$ decay ${}^{(}\overline{B}{}^{)}_s \to VV'$, where VV' is a superposition of CP eigenstates with vector mesons V, V', not only determines $\Delta\Gamma_s \cos(\phi_s^\Delta - 2\beta_s)$, but also contains information on $\sin(\phi_s^\Delta - 2\beta_s)$ through a CP-odd interference term. Here the golden mode is certainly ${}^{(}\overline{B}{}^{)}_s \to J/\psi\phi$, but also final states with higher ψ resonances and ${}^{(}\overline{B}{}^{)}_s \to D_s^{*+} D_s^{*-}$ can be studied. The determination of ϕ_s^Δ from the CP-odd interference term in untagged samples involves a four-fold ambiguity. It could be reduced to a two-fold ambiguity if the signs of $\cos\delta_1$ and $\cos\delta_2$ were determined, where δ_1 and δ_2 are the strong phases involved [44, 46]. These two solution are related by $\phi_s^\Delta \leftrightarrow \phi_s^\Delta \pm \pi$. If one relaxes the assumptions on $\cos\delta_1$ and $\cos\delta_2$, one is back to the same four-fold ambiguity as in item 2.

4. The branching fraction $Br({}^{(}\overline{B}{}^{)}_s \to D_s^{(*)+} D_s^{(*)-})$ approximates the width difference $\Delta\Gamma_{\rm CP}$ between the two CP eigenstates of the B_s system [44]. Irrespective of any new physics in M_{12}^s one always has $\Delta\Gamma_{\rm CP} = 2|\Gamma_{12}^s|$, so no constraint on our new physics parameter Δ_s is gained. Yet the ratio of $\Delta\Gamma_s \cos(\phi_s^\Delta - 2\beta_s)$ and $\Delta\Gamma_{\rm CP}$ could cleanly determine $\cos(\phi_s^\Delta)\cos(\phi_s^\Delta - 2\beta_s)$. However, $Br({}^{(}\overline{B}{}^{)}_s \to D_s^{(*)+} D_s^{(*)-})$ only equals $\Delta\Gamma_{\rm CP}$ in the poorly tested simultaneous limit of an infinitely heavy charm quark with small-velocity [47] and an infinite number of colours [48]. In order to test this limit one needs to measure the CP-odd and CP-even fractions of all $b \to c\overline{c}s$ decays [44]. Until this has been done nothing can be inferred from $Br({}^{(}\overline{B}{}^{)}_s \to D_s^{(*)+} D_s^{(*)-})$, in particular this quantity neither gives an upper bound (since other CP-even $b \to c\overline{c}s$ modes can be relevant) nor a lower bound (since other CP-odd $b \to c\overline{c}s$ modes can be relevant and the $D_s^{(*)+} D_s^{(*)-}$ final state has a CP-odd component) on $\Delta\Gamma_{\rm CP}$. We strongly discourage from the inclusion of $Br({}^{(}\overline{B}{}^{)}_s \to D_s^{(*)+} D_s^{(*)-})$ in averages with $\Delta\Gamma_s$ determined from clean methods.

5. $a_{\rm fs}^s$ can be measured from untagged flavour-specific ${}^{(}\overline{B}{}^{)}_s$ decays, typically from the number of positively and negatively charged leptons in semileptonic decays. Observing further the time evolution of these untagged ${}^{(}\overline{B}{}^{)}_s \to X^\mp \ell^\pm {}^{(}\overline{\nu}{}^{)}_\ell$ decays (see e.g. [8]),

$$\frac{\Gamma[{}^{(}\overline{B}{}^{)}_s \to X^- \ell^+ \nu_\ell, t] \,-\, \Gamma[{}^{(}\overline{B}{}^{)}_s \to X^+ \ell^- \overline{\nu}_\ell, t]}{\Gamma[{}^{(}\overline{B}{}^{)}_s \to X^- \ell^+ \nu_\ell, t] \,+\, \Gamma[{}^{(}\overline{B}{}^{)}_s \to X^+ \ell^- \overline{\nu}_\ell, t]} \;=\; \frac{a_{\rm fs}^s}{2}\left[1 - \frac{\cos(\Delta M_s\, t)}{\cosh\left(\Delta\Gamma_s\, t/2\right)}\right], \qquad (84)$$

will have two advantages: one can use the oscillatory behaviour to control fake effects from experimental detection asymmetries (which are constant in time) and to separate the B_s and B_d samples through $\Delta M_s \neq \Delta M_d$. The constraint from $a_{\rm fs}^s$ on Δ_s is given in Eq. (78). It defines a circle in the complex Δ_s plane which touches the x–axis at the origin. The constraint from $a_{\rm fs}^s$ on Δ_s only has a two-fold ambiguity (related to $\phi_s \leftrightarrow \pi - \phi_s$) and discriminates between the solutions in the upper and lower half–plane in Fig. 6.

6. The time dependence of the tagged decay $B_s \to J/\psi\phi$ permits the determination of the mixing-induced CP asymmetries $A_{\rm CP}^{\rm mix}(B_s \to (J/\psi\phi)_{CP\pm})$. The angular analysis separates the

CP–odd P-wave component from the CP–even S-wave and D-wave. The time-dependent CP asymmetry is (in the notation of [6, 44]):

$$\frac{\Gamma(\bar{B}_s^0(t) \to f) - \Gamma(B_s^0(t) \to f)}{\Gamma(\bar{B}_s^0(t) \to f) + \Gamma(B_s^0(t) \to f)} \;=\; -\frac{A_{CP}^{\rm mix} \sin(\Delta M_s t)}{\cosh(\Delta\Gamma_s t/2) + A_{\Delta\Gamma} \sinh(\Delta\Gamma_s t/2)}. \tag{85}$$

One finds $\phi_s^\Delta - 2\beta_s$ through

$$A_{\rm CP}^{\rm mix}(B_s \to (J/\psi\phi)_{CP\pm}) \;=\; \pm \sin(\phi_s^\Delta - 2\beta_s), \qquad A_{\Delta\Gamma} \;=\; \mp \cos(\phi_s^\Delta - 2\beta_s) \tag{86}$$

with the same two-fold ambiguity as from $a_{\rm fs}^s$ in item 5. Combining Eqs. (75) and (78) with Eq. (86) and neglecting the tiny contributions of $\phi_s^{\rm SM}$ and β_s one verifies the correlation between $a_{\rm fs}^s$ and $A_{\rm CP}^{\rm mix}(B_s \to (J/\psi\phi)_{CP\pm})$ derived in [12, 13]. In fact such correlations can be found between any three of the observables discussed above, because the $B_s - \overline{B}_s$ mixing only involves the two parameters $|\Delta_s|$ and ϕ_s.

An important remark here concerns the decay $B_s \to K^+K^-$, as one might be tempted to use the lifetime measured in $B_s \to K^+K^-$ to determine $\Gamma_s + |\Delta\Gamma_s/2|$. While K^+K^- is CP even, the decay is penguin–dominated and as such sensitive to the same kind of new physics which may be responsible for the experimental anomaly seen in penguin–dominated B_d decays [3]. Thus information from $B_s \to K^+K^-$ should under no circumstances be included in any averages with the measurements discussed above. Instead one should confront the lifetime measured in this mode with the one obtained from $B_s \to (J/\psi\phi)_{CP+}$ to probe new physics in $b \to s$ penguin decays.

For a visualisation of the bounds from Eqs. (75–78) in the complex Δ_s-plane we consider now the hypothetical case of $|\Delta_s| = 0.9$ and $\phi_s^\Delta = -\pi/4$. Suppose one would measure these central values:

$$\Delta M_s = 17.4\,{\rm ps}^{-1}, \qquad \Delta\Gamma_s = 0.068\,{\rm ps}^{-1}, \tag{87}$$

$$\frac{\Delta\Gamma_s}{\Delta M_s} = 3.91 \cdot 10^{-3}, \qquad a_{\rm fs}^s = -3.89 \cdot 10^{-3}\,. \tag{88}$$

Moreover we assume the following theoretical and experimental uncertainties: $\Delta M_s : \pm 15\%$, $\Delta\phi_s : \pm 20\%$, $\Delta\Gamma_s/\Delta M_s : \pm 15\%$, $a_{\rm fs}^s : \pm 20\%$. The regions in the Δ_s-plane bounded for these hypothetical measurements are shown in figure 6.

The constraints from CP-conserving quantities are symmetric to the Im(Δ_s)-axis, The bound from ΔM_s simply gives a circle with the origin (0,0) and the radius $|\Delta_s|$. In the measurement of $\Delta\Gamma_s$ we have assumed that the data are fitted to the correct formula Eq. (80) and $|\Delta\Gamma_s|$ and $|\cos(\phi_s - 2\beta_s)|$ have been determined as discussed above in item 2. In practice the extracted $|\Delta\Gamma_s|$ and $|\cos(\phi_s^\Delta - 2\beta_s)|$ are strongly correlated and mainly $|\Delta\Gamma_s||\cos(\phi_s^\Delta - 2\beta_s)|$ is determined (see Eq. (83) and [44]). The constraint from the hadronically cleaner ratio $|\Delta\Gamma_s|/\Delta M_s$ are two circles which touch the y–axis in the origin. If one fully includes the correlation between $|\Delta\Gamma_s|$ and $|\cos(\phi_s^\Delta - 2\beta_s)|$ one will rather find constraints which roughly correspond to a fixed $|\Delta\Gamma_s \cos(\phi_s^\Delta - 2\beta_s)|/\Delta M_s$. The corresponding curves are a bit more eccentric than the circles from $|\Delta\Gamma_s|/\Delta M_s$.

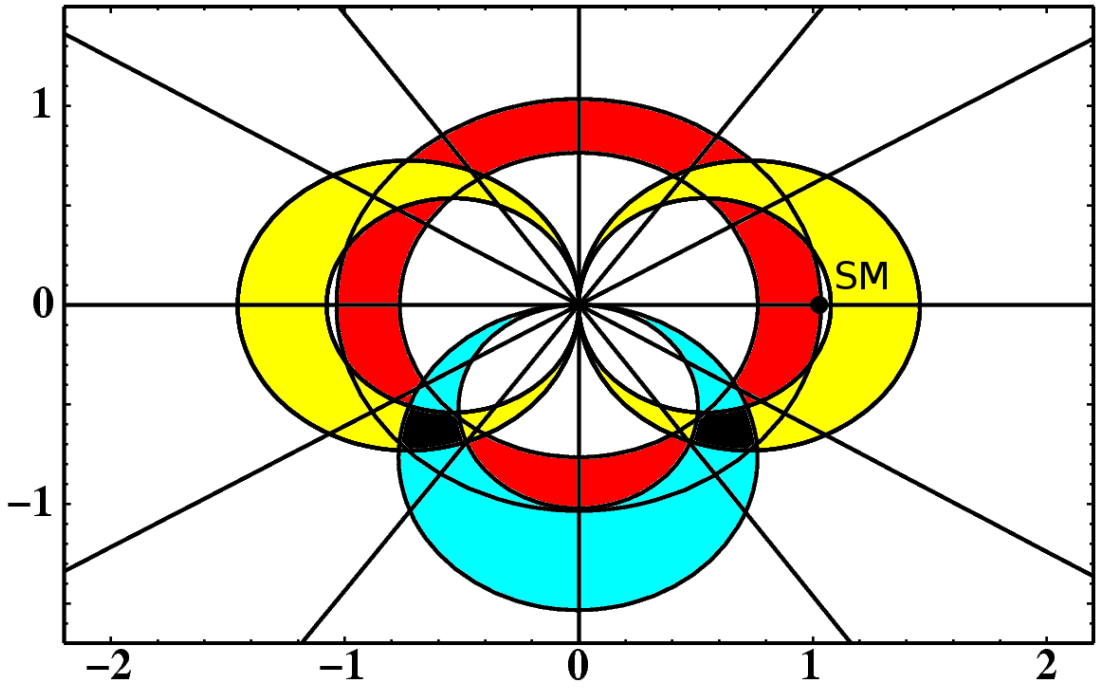

Figure 6: Illustration of the bounds in the complex Δ_s-plane for $|\Delta_s| = 0.9$ and $\phi_s^\Delta = -\pi/4$. We assume the following overall uncertainties: ΔM_s (red or dark-grey) : $\pm 15\%$, $\Delta\Gamma_s/\Delta M_s$ (yellow or light-grey): $\pm 15\%$, $a_{\rm fs}^s$ (light-blue or grey) : $\pm 20\%$ and ϕ_s^Δ (solid lines) : $\pm 20\%$.

If one plots the bounds from $|\Delta\Gamma_s|$ (or $|\Delta\Gamma_s \cos(\phi_s^\Delta - 2\beta_s)|$) alone, one finds four rays starting from the origin. The experimental information in this is redundant, as it is fully contained in the constraints from ΔM_s and $|\Delta\Gamma_s|/\Delta M_s$. For the theory uncertainties, however, this is not true: if (as current data do) ΔM_s prefers a small value of f_{B_s}, while $\Delta\Gamma_s$ prefers a large f_{B_s}, the combined constraint from ΔM_s and $|\Delta\Gamma_s|$ will exclude a region of the Δ_s plane which is allowed by the ratio $|\Delta\Gamma_s|/\Delta M_s$, from which f_{B_s} drops out.

The measurement of $a_{\rm fs}^s$ yields a circle touching the x–axis in the origin, in particular it reduces the four-fold ambiguity in the extracted value of Δ_s to a two-fold one. The extraction of $\phi_s^\Delta - 2\beta_s$ from the angular analysis in ${}^{(}\overline{B}{}_s^{)} \to J/\psi\phi$ (as discussed in item 3) also yields four rays starting from the origin (corresponding to the same value of $|\cos(\phi_s^\Delta - 2\beta_s)|$), if no assumptions on the signs of $\cos\delta_1$ and $\cos\delta_2$ are made. Finally, the measurement of $A_{\rm CP}^{\rm mix}(B_s \to (J/\psi\phi)_{CP\pm})$ will select two out of these four rays, discriminating between $\phi_s^\Delta - 2\beta_s > 0$ and $\phi_s^\Delta - 2\beta_s < 0$.

4.3 Current experimental constraints on Δ_s

In this section we turn to the real world and discuss the current experimental constraints on the complex Δ_s-plane. In view of the experimental errors we set β_s to zero and identify ϕ_s with ϕ_s^Δ.

The mass difference ΔM_s is now known very precisely [10], see Eq. (7). For the remaining mixing parameters in the B_s-system only weak experimental constraints are available. The only

available experimental analysis of $|\Delta\Gamma_s|$ with the correct implementation of the phase ϕ_s is from the DØ collaboration, their analysis in [49] was recently updated in [50] using 1fb^{-1} of data. Setting the value of the mixing phase ϕ_s to zero (Standard Model scenario) they obtain [50]

$$\Delta\Gamma_s \;=\; 0.12 \pm 0.08_{\text{(stat)}}\; {}^{+0.03}_{-0.04\,\text{(syst)}}\; \text{ps}^{-1}\,. \tag{89}$$

Allowing for a non-zero value of the mixing phase ϕ_s they get

$$\begin{aligned} \Delta\Gamma_s \;&=\; 0.17 \pm 0.09_{\text{(stat)}} \pm 0.03_{\text{(syst)}}\; \text{ps}^{-1} \\ &\text{and} \quad \phi_s \;=\; -0.79 \pm 0.56_{\text{(stat)}} \pm 0.01_{\text{(syst)}} \end{aligned} \tag{90}$$

$$\begin{aligned} \text{or} \qquad \Delta\Gamma_s \;&=\; -0.17 \pm 0.09_{\text{(stat)}} \pm 0.03_{\text{(syst)}}\; \text{ps}^{-1} \\ &\text{and} \quad \phi_s \;=\; -0.79 \pm 0.56_{\text{(stat)}} \pm 0.01_{\text{(syst)}} \;+\; \pi\,. \end{aligned} \tag{91}$$

As expected from Eq. (83) the values for $|\Delta\Gamma_s \cos\phi_s|$ found from Eqs. (89) and (91) are roughly equal to $\Delta\Gamma_s$ in Eq. (89). The quoted results in Eqs. (90) and (91) assume that the signs of $\cos\delta_1$ and $\cos\delta_2$ agree with the results found with naive factorisation. With this assumption the other two solutions for ϕ_s (which have opposite signs to those in Eqs. (90) and (91)) are excluded. Strategies to check this theoretical input are discussed in [44].

The semileptonic CP asymmetry $a^s_{\text{sl}} \equiv a^s_{\text{fs}}$ in the B_s system has been determined directly in [51] and was found to be

$$a_{\text{sl}}^{s,\text{direct}} = (24.5 \pm 19.3_{\text{(stat)}} \pm 3.5_{\text{(syst)}}) \cdot 10^{-3}\,. \tag{92}$$

Moreover the semileptonic CP asymmetry can be extracted from the same sign dimuon asymmetry that was measured in [52] as

$$a_{\text{sl}} = (-5.3 \pm 2.5_{\text{(stat)}} \pm 1.8_{\text{(syst)}}) \cdot 10^{-3} \tag{93}$$

in a data sample containing both B_d and B_s mesons. While the composition of the sample is known, no determination of the initial state on an event–by–event basis was possible. Updating the numbers in [14, 53] one sees that the measurement in Eq. (93) determines the combination

$$a_{\text{sl}} = (0.582 \pm 0.030)\; a^d_{\text{sl}} + (0.418 \pm 0.047)\; a^s_{\text{sl}}. \tag{94}$$

In [14, 53] the experimental bound for a^d_{sl} from B factories was used to extract a bound on a^s_{sl} from Eq.(93) and Eq.(94). The huge experimental uncertainty in a^d_{sl} then inflicts a large error on the value of a^s_{sl} inferred from Eqs. (93) and (94).

Here we pursue a different strategy and use the much more precise theoretical Standard Model value for a^d_{sl} in Eq. (71). In the search for new physics this is permissible: if the resulting constraint on Δ_s departs from the Standard Model value $\Delta_s = 1$, this will then imply new physics in either a^s_{sl} or a^d_{sl}. Moreover, the current precision in the unitarity triangle already substantially limits the room for new physics in a^d_{sl} [2].

Using $a^d_{\text{sl}} = -\left(0.48^{+0.10}_{-0.12}\right) \cdot 10^{-3}$ of Eq. (71) and further Eqs. (93) and (94) we obtain the nice bound

$$a_{\text{sl}}^{s,\text{dimuon}} = (-12.0 \pm 6.0_{\text{(stat)}} \pm 4.5_{\text{(syst)}}) \cdot 10^{-3}\,. \tag{95}$$

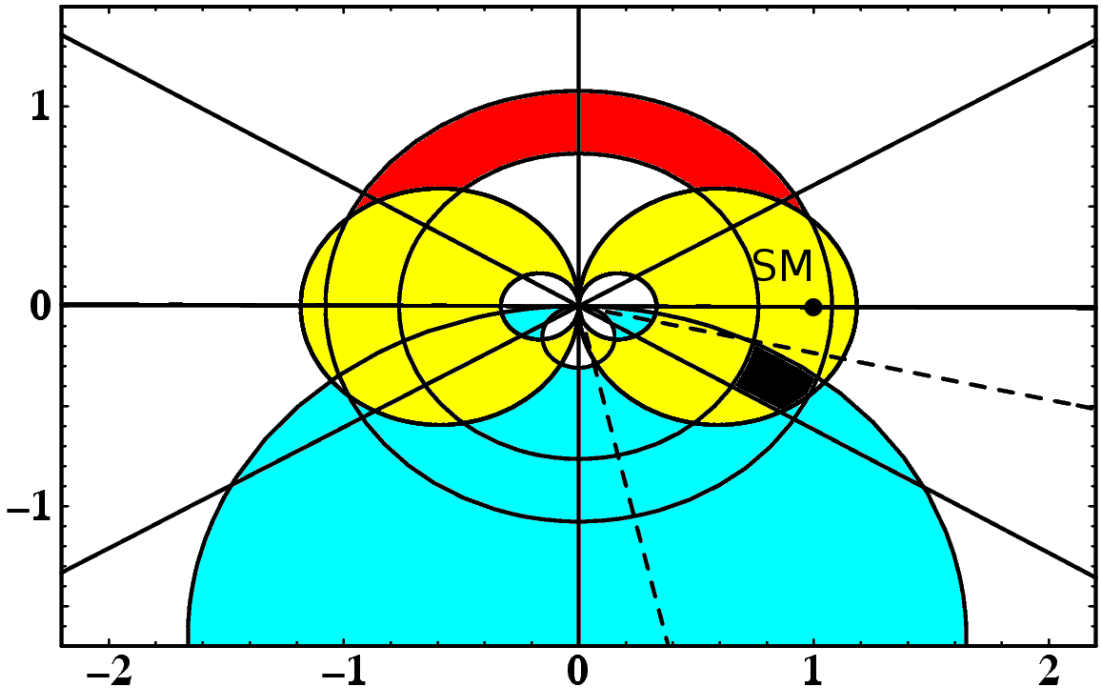

Figure 7: Current experimental bounds in the complex Δ_s-plane. The bound from ΔM_s is given by the red (dark-grey) annulus around the origin. The bound from $|\Delta\Gamma_s|/\Delta M_s$ is given by the yellow (light-grey) region and the bound from $a^s_{\rm fs}$ is given by the light-blue (grey) region. The angle ϕ_s^Δ can be extracted from $|\Delta\Gamma_s|$ (solid lines) with a four–fold ambiguity — each of the four regions is bounded by a solid ray and the x-axis — or from the angular analysis in $B_s \to J/\Psi\phi$ (dashed line). This constraint also has a four–fold ambiguity if no assumptions on the strong phases δ_1 and δ_2 are made. The dashed lines limit the region corresponding to the solution in Eq. (90). The Standard Model case corresponds to $\Delta_s = 1$. The current experimental situation shows a small deviation, which may become significant, if the experimental uncertainties in $\Delta\Gamma_s$, $a^s_{\rm sl}$ and ϕ_s will go down in near future.

Combining this number with the one from the direct determination [51] in Eq. (92) we get our final experimental number for the semileptonic CP asymmetry:

$$a^s_{\rm sl} = (-8.8 \pm 5.7_{\rm (stat)} \pm 4.5_{\rm (syst)}) \cdot 10^{-3}\,. \tag{96}$$

Adding statistical and systematic error in quadrature gives

$$a^s_{\rm sl} = (-8.8 \pm 7.3) \cdot 10^{-3}\,. \tag{97}$$

In Fig. (7) we display all bounds in the complex Δ_s-plane including all experimental and theoretical uncertainties.

The combined analysis of ΔM_s, ϕ_s, $|\Delta\Gamma_s|/\Delta M_s$ and $a^s_{\rm sl}$ in Fig. 7 shows some hints for deviations from the Standard Model. To analyse them further we ignore discrete ambiguities

and focus on the solution in the fourth quadrant which is closest to the Standard Model solution $\Delta_s = 1$. We further do not perform a complete statistical analysis with proper inclusion of all correlations and for simplicity add statistical and systematic errors in quadrature. First we note from Eq. (75) that Eq. (7) implies

$$|\Delta_s| \;=\; 0.92 \pm 0.32_{\text{(th)}} \pm 0.01_{\text{(exp)}} \tag{98}$$

while Eqs. (77) and (90) lead to

$$\frac{\cos\phi_s}{|\Delta_s|} \;=\; 1.93 \pm 0.37_{\text{(th)}} \pm 1.1_{\text{(exp)}}. \tag{99}$$

Eqs. (98) and (99) are consistent with $\Delta_s = 1$, but prefer $|\Delta_s| < 1$.

Second we observe that both the angular distribution in $\overset{(}{B}{}^{)}_s \to J/\psi\phi$ giving Eq. (91) and $a^s_{\rm sl}$ in Eq. (97) point towards a non-zero ϕ_s. Both analyses involve $\sin\phi_s$, the two values inferred are

$$\sin\phi_s \;=\; -0.71^{+0.48}_{-0.27} \qquad \text{from the angular analysis, Eq. (91),} \tag{100}$$

$$\frac{\sin\phi_s}{|\Delta_s|} \;=\; -1.77 \pm 0.33_{\text{(th)}} \pm 1.47_{\text{(exp)}} \qquad \text{from } a_{\rm sl} \text{ in Eq. (97).} \tag{101}$$

In Eq. (101) we have profited from our improved theory prediction in Eq. (78). For $|\Delta_s| = 1$ the two numbers combine to

$$\sin\phi_s \;=\; -0.77 \pm 0.02_{\text{(th)}} \pm 0.36_{\text{(exp)}}. \tag{102}$$

Relaxing $|\Delta_s|$ to its minimal value allowed by Eq. (98), $|\Delta_s| = 0.59$, changes this result to

$$\sin\phi_s \;=\; -0.76 \pm 0.03_{\text{(th)}} \pm 0.34_{\text{(exp)}}. \tag{103}$$

Either Eq. (102) or Eq. (103) alone imply a deviation from $\phi_s = 0$ by 2.1σ, but $\Delta\Gamma_s$ in Eq. (91) pulls in the opposite direction, preferring large values of $|\cos\phi_s|$ through Eq. (76). Despite of its large error $\Delta\Gamma_s$ already gives a powerful lower bound $|\cos\phi_s| \geq 0.55$ (so that $|\sin\phi_s| \leq 0.84$) at the 1σ level because of its large central value in Eq. (91). This can be clearly seen from Fig. 7. However, $\Delta\Gamma_s$ is consistent with $\cos\phi_s = 0$ at the 1.8σ level and clearly has no impact on the small ϕ_s region, which is the relevant region to assess the significance of Eq. (102) in the search for new physics.

In conclusion we find that the data are best fit for ϕ_s around -0.88 corresponding to $\sin\phi_s = -0.77$, if $|\Delta_s| = 1$. The constraint from $|\Delta\Gamma_s|$ is less compelling, but slightly prefers $|\Delta_s| < 0$ and disfavours too large values of $|\sin\phi_s|$. The discrepancy between data and the Standard Model is around 2σ, which is not statistically significant yet. If our results are used to constrain models of new physics one should bear in mind that we have only discussed the solution in the fourth quadrant of the complex Δ_s plane here.

5 A road map for $B_s - \overline{B}_s$ mixing

Clearly the best way to establish new physics from $B_s - \overline{B}_s$ mixing is a combination of all observables following the line of Sect. 4.2. In particular it has to be stressed that $A_{\rm CP}^{\rm mix}(B_s \to (J/\psi\phi)_{CP\pm})$ and $a_{\rm fs}^s$ are not substitutes for each other, but rather give complementary information on the complex Δ_s plane because of their different dependence on $|M_{12}^s|$. With the new operator basis presented in this paper it will be possible to determine Δ_s solely from measurements which involve hadronic quantities only in numerically sub-dominant terms. To this end any experimental progress on $|\Delta\Gamma_s|$, $a_{\rm fs}^s$, the angular distributions of both untagged and tagged $B_s \to J/\psi\phi$ decays (with the tagged analysis giving access to $A_{\rm CP}^{\rm mix}(B_s \to (J/\psi\phi)_{CP\pm})$) and possibly of other $b \to c\bar{c}s$ decays of the B_s meson is highly desirable. Regardless of whether $\sin\phi_s$ turns out to be zero or not it is important to measure the sign of $\Delta\Gamma_s$. Methods for this are discussed in [44]. Probably the most promising way to determine sign $\Delta\Gamma_s = $ sign $\cos(\phi_s)$ is the study of $B_s \to J/\psi K^+K^-$ with a scan of the invariant mass of the (K^+, K^-) pair around the ϕ peak to determine sign $\cos\delta_{1,2}$.

Clearly the analysis of the precise measurement of ΔM_s needs a better determination of $f_{B_s}^2 B$. Since any new physics discovery from a quantity involving lattice QCD will be met with scepticism by the scientific community, the lattice collaborations might want to consider to switch to blind analyses in the future. The predictions of both $\Delta\Gamma_s/\Delta M_s$ and $a_{\rm fs}^s$ involve the ratio $\tilde{B}_S'/B$ in a numerically sub-dominant term. It may be worthwhile to address this ratio directly in lattice computations, because some systematic effects could drop out from the ratio of the two matrix elements.

The quantities discussed in this paper will also profit from higher-order calculations of the short-distance QCD parts. In particular corrections of order α_s/m_b should be computed to permit a meaningful use of $1/m_b$ bag factors computed with lattice QCD or QCD sum rules. A further reduction of the dependence on the renormalisation scale μ_1 requires the cumbersome calculation of $\mathcal{O}(\alpha_s^2)$ corrections. Finally, the reduction of the $1/m_b$ corrections with the help of our new operator basis can only be fully appreciated, if the size of the $1/m_b^2$ terms is indeed small. We have estimated these corrections and indeed found no unnatural enhancement over their natural size.

6 Summary

In this letter we have improved the theoretical accuracy of the mixing quantity Γ_{12}^q, $q = d, s$, by summing the logarithmic terms $\alpha_s^n z \ln^n z$, $z = m_c^2/m_b^2$ to all orders $n = 1, 2, \ldots$ and by introducing a new operator basis, which trades the traditionally used operator Q_S of Eq. (8) for $\widetilde{Q}_S$ defined in Eq. (16). In the new operator basis the coefficient of the $1/m_b$–operator R_0 is colour–suppressed. We have found that all previously noted pathologies in the sizes of the $1/m_b$ and α_s corrections were artifacts of the old operator basis. Still, one could achieve the same accuracy with the use of the old basis, if one i) used the coefficients with resummed $\ln z$ terms, ii) added the term of order $N_c\alpha_s/m_b$ which drops from the NLO results of [19–21] when $\widetilde{Q}_S$ is eliminated for R_0 and iii) fully takes the numerical correlation between B and B_S into account.

This numerical correlation stems from the smallness of the matrix element $\langle \widetilde{Q}_S \rangle$. It is most easily implemented by expressing either B or B_S in terms of $\widetilde{B}_S$, which is essentially equivalent to our approach.

Our improvements are most relevant for $\mathrm{Re}\,\Gamma_{12}^q/M_{12}^q$, which enters both $\Delta\Gamma_q/\Delta M_q$ and new physics scenarios of $a_{\rm fs}^s$. In particular, hadronic quantities now appear in these quantities in numerically sub-dominant terms only. We have then discussed how experimental information on $|\Delta\Gamma_s|$, $a_{\rm fs}^s$, ϕ_s from the angular distribution of $\overline{(B_s)} \to J/\psi\phi$ and $A_{\rm CP}^{\rm mix}(B_s \to (J/\psi\phi)_{CP\pm})$ can be efficiently combined to constrain the complex parameter Δ_s, which quantifies new physics in $B_s - \overline{B}_s$ mixing.

Armed with our more precise formulae we have analysed the combined impact of the DØ analyses of the dimuon asymmetry and of the angular distribution in the decay $\overline{(B_s)} \to J/\psi\phi$. Here we have assumed that ϕ_d is free of new physics contributions. This is plausible in view of the constraints on ϕ_d from global fits to the unitarity triangle [2]. Scanning conservatively over theory uncertainties, we find that ϕ_s deviates from its Standard Model value by 2 standard deviations.

Acknowledgements

This paper has substantially benefited from discussions with Damir Becirevic, Guennadi Borissov, Sandro De Cecco, Jonathan Flynn, Bruce Hoeneisen, Heiko Lacker, Vittorio Lubicz, Alexei Pivovarov, Junko Shigemitsu, Cecilia Tarantino, Wolfgang Wagner, Matthew Wingate, Norikazu Yamada and Daria Zieminska. A.L. thanks the University of Karlsruhe for several invitations and U.N. thanks the Fermilab theory group for hospitality. We are grateful to Franz Stadler for preparing the pie charts. We thank Luca Silvestrini for pointing out our incorrect use of the experimental input on the dimuon asymmetry in eq. (93).

This work was supported in part by the DFG grant No. NI 1105/1–1, by the EU Marie-Curie grant MIRG–CT–2005–029152, by the BMBF grant 05 HT6VKB and by the EU Contract No. MRTN-CT-2006-035482, “FLAVIAnet”.

References

[1] N. Cabibbo, Phys. Rev. Lett. **10**, 531 (1963); M. Kobayashi and T. Maskawa, Prog. Theor. Phys. **49**, 652 (1973).

[2] Updated result of J. Charles *et al.* [CKMfitter Group], Eur. Phys. J. C **41** (2005) 1 [arXiv:hep-ph/0406184] for the summer conferences 2006, see http://www.slac.stanford.edu/xorg/ckmfitter/ckm_results_beauty2006.html; updated result of M. Bona *et al.* [UTfit Collaboration], arXiv:hep-ph/0606167 for the summer conferences 2006, see http://utfit.roma1.infn.it/; updated result of E. Barberio *et al.* [Heavy Flavor Averaging Group (HFAG)], arXiv:hep-ex/0603003 for the summer conferences 2006, see http://www.slac.stanford.edu/xorg/hfag/.

[3] The experimental situation is summarised in: M. Hazumi, plenary talk at *33rd International Conference On High Energy Physics (ICHEP 06)*, 26 Jul – 2 Aug 2006, Moscow, Russia.

[4] D. Chang, A. Masiero and H. Murayama, Phys. Rev. D **67**, 075013 (2003) [arXiv:hep-ph/0205111].

[5] Effects of the model in [4] on $B_s - \overline{B}_s$ mixing have been studied in: S. Jäger and U. Nierste, Eur. Phys. J. C **33**, S256 (2004) [arXiv:hep-ph/0312145]; S. Jäger and U. Nierste, in *Proceedings of the 12th International Conference On Supersymmetry And Unification Of Fundamental Interactions (SUSY 04)*, 17-23 Jun 2004, Tsukuba, Japan, p. 675-678, Ed. K. Hagiwara, J. Kanzaki, N. Okada [hep-ph/0410360]; S. Jäger, hep-ph/0505243, to appear in the *Proceedings of the XLth Rencontres de Moriond, Electroweak Interactions and Unified Theories*, 5-12 Mar 2005, La Thuile, Aosta Valley, Italy, Ed. J. Tran Thanh Van.

[6] K. Anikeev *et al.*, *B physics at the Tevatron: Run II and beyond*, [hep-ph/0201071], Chapters 1.3 and 8.3.

[7] E. H. Thorndike, Ann. Rev. Nucl. Part. Sci. 35 (1985) 195; J. S. Hagelin and M. B. Wise, Nucl. Phys. B **189** (1981) 87; J. S. Hagelin, Nucl. Phys. B **193** (1981) 123; A. J. Buras, W. Slominski and H. Steger, Nucl. Phys. B **245** (1984) 369. R. N. Cahn and M. P. Worah, Phys. Rev. D **60** (1999) 076006;

[8] U. Nierste, [hep-ph/0406300], in: *Proceedings of the XXXIXth Rencontres de Moriond, Electroweak Interactions and Unified Theories*, 21-28 Mar 2004, La Thuile, Aosta Valley, Italy, Ed. J. Tran Thanh Van.

[9] A.J. Buras, M. Jamin and P.H. Weisz, Nucl. Phys. **B347**, 491 (1990).

[10] A. Abulencia *et al.* [CDF Collaboration], arXiv:hep-ex/0609040; A. Abulencia [CDF - Run II Collaboration], Phys. Rev. Lett. **97** (2006) 062003 [arXiv:hep-ex/0606027]; V. M. Abazov *et al.* [DØ Collaboration], Phys. Rev. Lett. **97** (2006) 021802 [arXiv:hep-ex/0603029].

[11] M. Ciuchini and L. Silvestrini, Phys. Rev. Lett. **97**, 021803 (2006) [arXiv:hep-ph/0603114]; M. Endo and S. Mishima, Phys. Lett. B **640** (2006) 205 [arXiv:hep-ph/0603251]; Z. Ligeti, M. Papucci and G. Perez, Phys. Rev. Lett. **97** (2006) 101801 [arXiv:hep-ph/0604112]; J. Foster, K. i. Okumura and L. Roszkowski, arXiv:hep-ph/0604121; P. Ball and R. Fleischer, arXiv:hep-ph/0604249; G. Isidori and P. Paradisi, Phys. Lett. B **639**, 499 (2006) [arXiv:hep-ph/0605012]; S. Khalil, Phys. Rev. D **74** (2006) 035005 [arXiv:hep-ph/0605021]; A. Datta, Phys. Rev. D **74** (2006) 014022 [arXiv:hep-ph/0605039]; S. Baek, JHEP **0609** (2006) 077 [arXiv:hep-ph/0605182]; X. G. He and G. Valencia, Phys. Rev. D **74** (2006) 013011 [arXiv:hep-ph/0605202]; R. Arnowitt, B. Dutta, B. Hu and S. Oh, Phys. Lett. B **641** (2006) 305 [arXiv:hep-ph/0606130]; S. Baek, J. H. Jeon and C. S. Kim, Phys. Lett. B **641** (2006) 183 [arXiv:hep-ph/0607113]; B. Dutta and Y. Mimura, arXiv:hep-ph/0607147; S. Chang,

C. S. Kim and J. Song, arXiv:hep-ph/0607313; F. J. Botella, G. C. Branco and M. Nebot, arXiv:hep-ph/0608100; S. Nandi and J. P. Saha, arXiv:hep-ph/0608341; G. Xiangdong, C. S. Li and L. L. Yang, arXiv:hep-ph/0609269; R. M. Wang, G. R. Lu, E. K. Wang and Y. D. Yang, arXiv:hep-ph/0609276; L. x. Lu and Z. j. Xiao, arXiv:hep-ph/0609279; M. Blanke and A. J. Buras, arXiv:hep-ph/0610037.

[12] M. Blanke, A. J. Buras, D. Guadagnoli and C. Tarantino, arXiv:hep-ph/0604057; M. Blanke, A. J. Buras, A. Poschenrieder, C. Tarantino, S. Uhlig and A. Weiler, arXiv:hep-ph/0605214;

[13] Z. Ligeti, M. Papucci and G. Perez, Phys. Rev. Lett. **97** (2006) 101801 [arXiv:hep-ph/0604112];

[14] Y. Grossman, Y. Nir and G. Raz, Phys. Rev. Lett. **97** (2006) 151801 [arXiv:hep-ph/0605028].

[15] Talks by D. Glenzinski (plenary), T. Moulik and S. Giagu at *33rd International Conference On High Energy Physics (ICHEP 06)*, 26 Jul – 2 Aug 2006, Moscow, Russia.

[16] A.J. Buras, M. Jamin, M.E. Lautenbacher and P.H. Weisz, Nucl. Phys. **B370**, 69 (1992); Addendum-ibid. **B375**, 501 (1992). M. Ciuchini, E. Franco, G. Martinelli, L. Reina, Nucl. Phys. **B415**, 403 (1994).

[17] E. Franco, M. Lusignoli and A. Pugliese, Nucl. Phys. **B194**, 403 (1982); L.L. Chau, Phys. Rep. **95**, 1 (1983); M.B. Voloshin, N.G. Uraltsev, V.A. Khoze and M.A. Shifman, Sov. J. Nucl. Phys. **46**, 112 (1987); A. Datta, E.A. Paschos and U. Türke, Phys. Lett. **B196**, 382 (1987); A. Datta, E.A. Paschos and Y.L. Wu, Nucl. Phys. **B311**, 35 (1988).

[18] M. Beneke, G. Buchalla and I. Dunietz, Phys. Rev. **D54**, 4419 (1996).

[19] M. Beneke, G. Buchalla, C. Greub, A. Lenz and U. Nierste, Phys. Lett. B **459** (1999) 631 [arXiv:hep-ph/9808385].

[20] M. Ciuchini, E. Franco, V. Lubicz, F. Mescia and C. Tarantino, JHEP **0308** (2003) 031 [arXiv:hep-ph/0308029].

[21] M. Beneke, G. Buchalla, A. Lenz and U. Nierste, Phys. Lett. B **576** (2003) 173 [arXiv:hep-ph/0307344].

[22] D. Becirevic, V. Gimenez, G. Martinelli, M. Papinutto and J. Reyes, JHEP **0204** (2002) 025 [arXiv:hep-lat/0110091].

[23] A. S. Dighe, T. Hurth, C. S. Kim and T. Yoshikawa, Nucl. Phys. B **624** (2002) 377 [arXiv:hep-ph/0109088].

[24] E. Dalgic *et al.*, arXiv:hep-lat/0610104; J. Shigemitsu for HPQCD Collaboration, talk at LATTICE 2006, http://www.physics.utah.edu/lat06/abstracts/sessions/weak/s1//Shigemitsu_Junko.pdf.

[25] M. Beneke, G. Buchalla, C. Greub, A. Lenz and U. Nierste, Nucl. Phys. B **639** (2002) 389 [arXiv:hep-ph/0202106].

[26] B. Aubert *et al.* [BABAR Collaboration], Phys. Rev. Lett. **93** (2004) 011803 [arXiv:hep-ex/0404017]. G. Corcella and A. H. Hoang, Nucl. Phys. Proc. Suppl. **133** (2004) 186 [arXiv:hep-ph/0311004]. M. Eidemuller, Phys. Rev. D **67** (2003) 113002 [arXiv:hep-ph/0207237]. J. H. Kuhn and M. Steinhauser, Nucl. Phys. B **619** (2001) 588 [Erratum-ibid. B **640** (2002) 415] [arXiv:hep-ph/0109084]. P. A. Baikov, K. G. Chetyrkin and J. H. Kuhn, Phys. Rev. Lett. **95** (2005) 012003 [arXiv:hep-ph/0412350]. E. Gamiz, M. Jamin, A. Pich, J. Prades and F. Schwab, arXiv:hep-ph/0505122. S. Narison, Phys. Lett. B **626**, 101 (2005) [arXiv:hep-ph/0501208]. E. Brubaker *et al.* [Tevatron Electroweak Working Group], arXiv:hep-ex/0608032.

[27] W. M. Yao *et al.* [Particle Data Group], J. Phys. G **33** (2006) 1.

[28] S. Bethke, arXiv:hep-ex/0606035.

[29] M. Jamin and B. O. Lange, Phys. Rev. D **65** (2002) 056005 [arXiv:hep-ph/0108135].

[30] J. G. Korner, A. I. Onishchenko, A. A. Petrov and A. A. Pivovarov, Phys. Rev. Lett. **91** (2003) 192002 [arXiv:hep-ph/0306032].

[31] C. S. Huang, A. Zhang and S. L. Zhu, Eur. Phys. J. C **21** (2001) 313 [arXiv:hep-ph/0011145].

[32] S. Hashimoto and T. Onogi, arXiv:hep-ph/0407221; S. Hashimoto, Int. J. Mod. Phys. A **20** (2005) 5133 [arXiv:hep-ph/0411126]; M. Okamoto, PoS **LAT2005** (2006) 013 [arXiv:hep-lat/0510113].

[33] A. Ali Khan *et al.* [CP-PACS Collaboration], Phys. Rev. D **64** (2001) 054504 [arXiv:hep-lat/0103020]; A. Ali Khan *et al.* [CP-PACS Collaboration], Phys. Rev. D **64** (2001) 034505 [arXiv:hep-lat/0010009]; C. Bernard *et al.* [MILC Collaboration], Phys. Rev. D **66** (2002) 094501 [arXiv:hep-lat/0206016]; S. Collins, C. T. H. Davies, U. M. Heller, A. Ali Khan, J. Shigemitsu, J. H. Sloan and C. Morningstar, Phys. Rev. D **60** (1999) 074504 [arXiv:hep-lat/9901001].

[34] S. Aoki *et al.* [JLQCD Collaboration], Phys. Rev. Lett. **91** (2003) 212001 [arXiv:hep-ph/0307039].

[35] V. Gimenez and J. Reyes, Nucl. Phys. Proc. Suppl. **94** (2001) 350 [arXiv:hep-lat/0010048].

[36] N. Yamada *et al.* [JLQCD Collaboration], Nucl. Phys. Proc. Suppl. **106** (2002) 397 [arXiv:hep-lat/0110087].

[37] M. Wingate, C. T. H. Davies, A. Gray, G. P. Lepage and J. Shigemitsu, Phys. Rev. Lett. **92** (2004) 162001 [arXiv:hep-ph/0311130]; A. Gray *et al.* [HPQCD Collaboration], Phys. Rev. Lett. **95** (2005) 212001 [arXiv:hep-lat/0507015].

[38] M. Beneke and A. Lenz, J. Phys. G **27** (2001) 1219 [arXiv:hep-ph/0012222].

[39] U. Nierste, in *Proc. of the 5th International Symposium on Radiative Corrections (RADCOR 2000)* ed. Howard E. Haber, arXiv:hep-ph/0105215;

[40] A. Lenz, arXiv:hep-ph/0412007;

[41] M. Bona *et al.* [UTfit Collaboration], arXiv:hep-ph/0605213.

[42] Y. Grossman, Y. Nir and M. P. Worah, Phys. Lett. B **407** (1997) 307 [arXiv:hep-ph/9704287].

[43] Y. Grossman, Phys. Lett. B **380** (1996) 99 [arXiv:hep-ph/9603244].

[44] I. Dunietz, R. Fleischer and U. Nierste, Phys. Rev. D **63** (2001) 114015 [arXiv:hep-ph/0012219].

[45] K. Hartkorn and H. G. Moser, Eur. Phys. J. C **8** (1999) 381.

[46] A. S. Dighe, I. Dunietz, H. J. Lipkin and J. L. Rosner, Phys. Lett. B **369** (1996) 144 [arXiv:hep-ph/9511363]. A. S. Dighe, I. Dunietz and R. Fleischer, Eur. Phys. J. C **6** (1999) 647 [arXiv:hep-ph/9804253].

[47] M. A. Shifman and M. B. Voloshin, Sov. J. Nucl. Phys. **47** (1988) 511 [Yad. Fiz. **47** (1988) 801].

[48] R. Aleksan, A. Le Yaouanc, L. Oliver, O. Pene and J. C. Raynal, Phys. Lett. B **316** (1993) 567.

[49] D. Acosta *et al.* [CDF Collaboration], Phys. Rev. Lett. **94** (2005) 101803 [arXiv:hep-ex/0412057]; DØ collaboration, conference note 5052, http://www-do.fnal.gov/.

[50] V. M. Abazov *et al.* [D0 Collaboration], Phys. Rev. Lett. **98** (2007) 121801 [arXiv:hep-ex/0701012].

[51] V. M. Abazov *et al.* [D0 Collaboration], arXiv:hep-ex/0701007.

[52] V. M. Abazov *et al.* [D0 Collaboration], Phys. Rev. D **74** (2006) 092001 [arXiv:hep-ex/0609014].

[53] G. Borissov, D. Zieminska and A. Chandra, DØ conference note no. 5189, http://www-do.fnal.gov. For an update see: V. Abazov *et al.* [D0 Collaboration], arXiv:hep-ex/0702030.